Chapter 9

Seismic Design of Steel Structures

Chia-Ming Uang, Ph.D.
Professor of Structural Engineering, University of California, San Diego

Michel Bruneau, Ph.D., P.Eng.
Professor of Civil Engineering, State University of New York at Buffalo

Andrew S. Whittaker, Ph.D., S.E.
Associate Professor of Civil Engineering, State University of New York at Buffalo

Key-Chyuan Tsai, Ph.D., S.E.
Professor of Civil Engineering, National Taiwan University

Key words: Seismic Design, Steel Structures, NEHRP Recommended Seismic Provisions, AISC Seismic Provisions, *R* Factor, Ductility, System Overstrength, Capacity Design, 1994 Northridge Earthquake, Moment-Resisting Frames, Brittle Fracture, Moment Connections, Concentrically Braced Frames, Buckling, Braces, Eccentrically Braced Frames, Links.

Abstract: Seismic design of steel building structures has undergone significant changes since the Northridge, California earthquake in 1994. Steel structures, thought to be ductile for earthquake resistance, experienced brittle fracture in welded moment connections. The latest AISC Seismic Provisions reflect the significant research findings that resulted from the Northridge earthquake. This chapter first starts with a description of the seismic design philosophy, the concept of system parameters (R, C_d, and Ω_o) and capacity design. Background information for the seismic requirements in the AISC Seismic Provisions of Moment Frames, Concentrically Braced Frames, and Eccentrically Braced Frames are then presented. Design examples are provided for each of the three structural systems.

9.1 Introduction

9.1.1 General

Steel is one of the most widely used materials for building construction in North America. The inherent strength and toughness of steel are characteristics that are well suited to a variety of applications, and its high ductility is ideal for seismic design. To utilize these advantages for seismic applications, the design engineer has to be familiar with the relevant steel design provisions and their intent and must ensure that the construction is properly executed. This is especially important when welding is involved.

The seismic design of building structures presented in this chapter is based on the NEHRP Recommended Provisions for the Development of Seismic Regulation for New Buildings (BSSC 1997). For seismic steel design, the NEHRP Recommended Provisions incorporate by reference the AISC Seismic Provisions for Structural Steel Buildings (1997b).

9.1.2 NEHRP Seismic Design Concept

The NEHRP Recommended Provisions are based on the *R*-factor design procedure. In this procedure, certain structural components are designated as the structural fuses and are specially detailed to respond in the inelastic range to dissipate energy during a major earthquake. Since these components are expected to experience significant damage, their locations are often selected such that the damage of these components would not impair the gravity load-carrying capacity of the system. Aside from these energy dissipating components, all other structural components including connections are then proportioned following the capacity design concept to remain in the elastic range.

Consider a structural response envelope shown in Figure 9-1, where the abscissa and ordinate represent the story drift and base shear ratio, respectively. If the structure is designed to respond elastically during a major earthquake, the required elastic base shear ratio, C_{eu}, would be high. For economical reasons, the NEHRP Recommended Provisions take advantage of the structure's inherent energy dissipation capacity by specifying a design seismic force level, C_s, which is reduced significantly from C_{eu} by a response modification factor, R:

$$C_s = \frac{C_{eu}}{R} \tag{9-1}$$

The C_s design force level is the first significant yield level of the structure, which corresponds to the force level beyond which the structural response starts to deviate significantly from the elastic response. Idealizing the actual response envelope by a linearly elastic-perfectly plastic response shown in Figure 9-1, it can be shown that the R factor is composed of two contributing factors (Uang 1991):

$$R = R_\mu \Omega_o \tag{9-2}$$

The ductility reduction factor, R_μ, accounts for the reduction of seismic forces from C_{eu} to C_y, Such a force reduction is possible because ductility, which is measured by the ductility factor μ (= δ_s/δ_y), is provided by the energy-dissipating components in the structural system.

The system overstrength factor, Ω_o, in Eq. 9-2 accounts for the reserve strength between the force levels C_y and C_s. Several factors contribute to this overstrength factor. These include structural redundancy, story drift limits, material overstrength, member oversize, non-seismic load combinations, and so on.

The *R*-factor design approach greatly simplifies the design process because the design engineer only has to perform an elastic structural analysis even though the structure is expected to deform well into the inelastic range during a major earthquake. After the elastic story drift, δ_e, is computed from a structural analysis, the NEHRP Recommended Provisions then specify a deflection amplification factor,

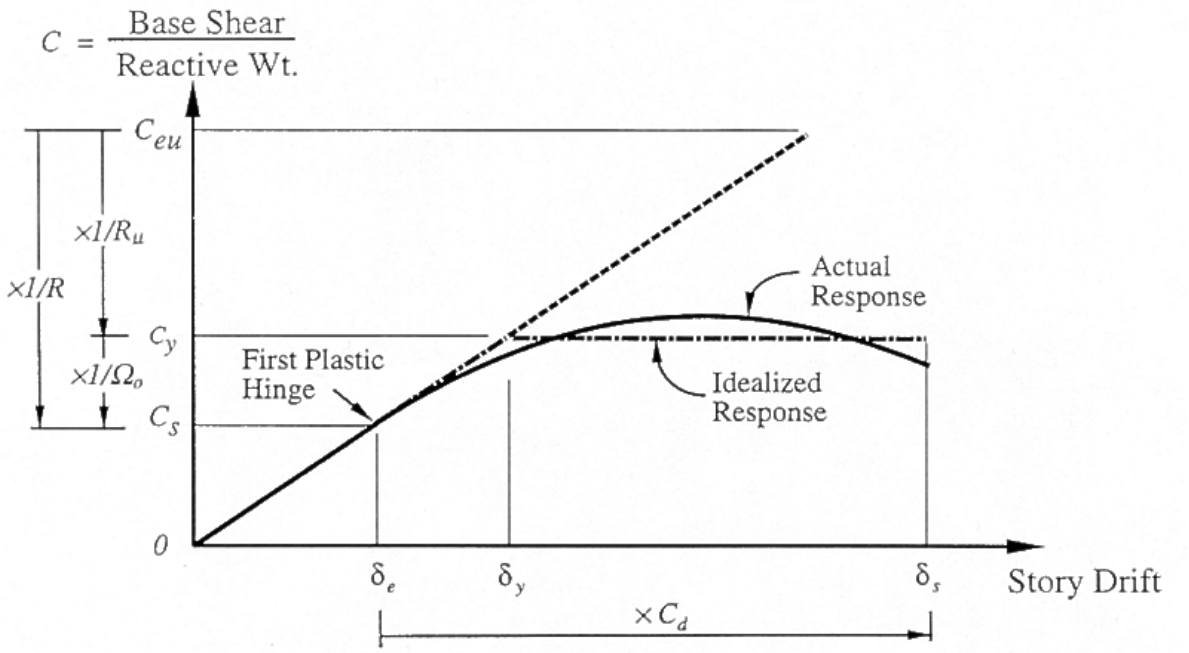

Figure 9-1. General structural response envelope

C_d, to estimate the Design Story Drift, δ_s, in Figure 9-1:

$$\delta_s = \frac{C_d \delta_e}{I} \qquad (9\text{-}3)$$

where I is the Occupancy Importance Factor. The story drift thus computed cannot exceed the allowable drift specified in the NEHRP Recommended Provisions. Depending on the Seismic Use Group, the allowable drift for steel buildings varies from 1.5% to 2.5% of the story height.

Note that the ultimate strength of the structure (C_y in Figure 9-1) is not known if only an elastic analysis is performed at the C_s design force level. Nevertheless, the ultimate strength of the structure is required in capacity design to estimate, for example, the axial force in the columns when a yield mechanism forms in the structure. For this purpose, the NEHRP Recommended Provisions specify Ω_o values to simplify the design process. Therefore, in addition to the load combinations prescribed in the AISC LRFD Specification (1993), the AISC Seismic Provisions require that the columns be checked for two additional special load combinations using the amplified horizontal earthquake load effects, $\Omega_o E$:

$$1.2D + 0.5L + 0.2S + \Omega_o E \qquad (9\text{-}4)$$

$$0.9D - \Omega_o E \qquad (9\text{-}5)$$

The amplified seismic load effects are to be applied without consideration of any concurrent bending moment on the columns. In addition, the required strengths determined from these two load combinations need not exceed either (1) the maximum load transferred to the column considering $1.1R_y$ times the nominal strengths of the connecting beam or brace elements of the frame, or (2) the limit as determined by the resistance of the foundation to uplift. Refer to the next section for the factor R_y.

The R, C_d, and Ω_o values specified in the NEHRP Recommended Provisions for different types of steel framing systems are listed in

Table 9-1. Steel framing systems and design parameters (NEHRP 1997)

Frame System	R	Ω_o	C_d
Bearing Wall Systems			
Ordinary Concentrically Braced Frames (OCBFs)	4	2	3 ½
Building Frame Systems			
Eccentrically Braced Frames (EBFs)			
• Moment connections at columns away from links	8	2	4
• Non-moment connections at columns away from links	7	2	4
Special Concentrically Braced Frames (SCBFs)	6	2	5
Ordinary Concentrically Braced Frames(OCBFs)	5	2	4 ½
Moment Resisting Frame Systems			
Special Moment Frames (SMFs)	8	3	5 ½
Intermediate Moment Frames (IMFs)	6	3	5
Ordinary Moment Frames (OMFs)	4	3	3 ½
Special Truss Moment Frames (STMFs)	7	3	5 ½
Dual Systems with SMFs Capable of Resisting at Least 25% of Prescribed Seismic Forces			
Eccentrically Braced Frames (EBFs)			
• Moment connections at columns away from links	8	2 ½	4
• Non-moment connections at columns away from links	7	2 ½	4
Special Concentrically Braced frames (SCBFs)	8	2 ½	6 ½
Ordinary Concentrically Braced Frames (OCBFs)	6	2 ½	5

Table 9-1. Seismic design of three widely used systems (moment-resisting frames, concentrically braced frames, and eccentrically braced frames) that are presented later in this chapter makes use of these parameters.

9.1.3 Structural Steel Materials

The ductility of steel generally reduces with an increase of the yield stress. Therefore, the AISC Seismic Provisions permit only the following grades of steel for seismic design: ASTM A36, A53, A500 (Grades B and C), A501, A572 (Grades 42 or 50), A588, A913 (Grade 50 or 65), or A992. Further, for those structural members that are designed to yield under load combinations involving Ω_o times the design seismic forces, the specified minimum yield strength, F_y, shall not exceed 50 ksi unless the suitability of the material is determined by testing or other rational criteria. This limitation does not apply to columns of A588 or A913 Grade 65 steel for which the only expected inelastic behavior is yielding at the column base.

The specified minimum yield strength is used to design the structural components that are expected to yield during the design earthquake. However, to estimate the force demand these components would impose on other structural components (including connections) that are expected to remain elastic, the expected yield strength, F_{ye}, of the energy dissipating components needs to be used for capacity design:

$$F_{ye} = R_y F_y \tag{9-6}$$

For rolled shapes and bars, the AISC Seismic Provisions stipulate that R_y shall be taken as 1.5 for A36 and 1.3 for A572 Grade 42. For rolled shapes and bars of other grades of steel and for plates, R_y shall be taken as 1.1 (SSPC 1995).

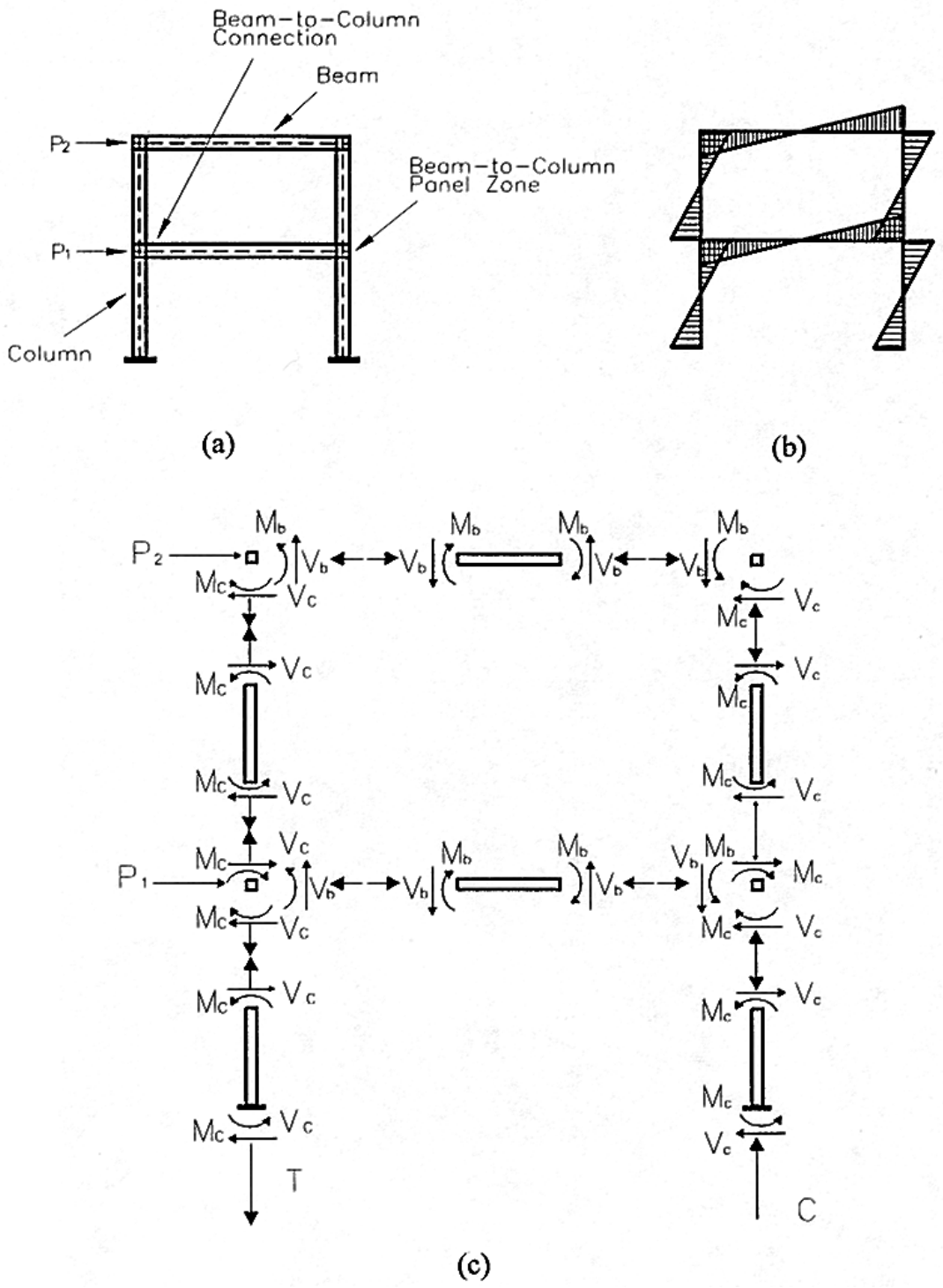

Figure 9-2. (a) Geometry considering finite dimensions of members, (b) Typical moment diagram under lateral loading, and (c) Corresponding member forces on beams, columns, and panel zones

9.2 Behavior and Design of Moment-Resisting Frames

9.2.1 Introduction

Steel moment-resisting frames (SMFs) are rectilinear assemblies of columns and beams that are typically joined by welding or high-strength bolting or both. Resistance to lateral loads is provided by flexural and shearing actions in the beams and the columns. Lateral stiffness is provided by the flexural stiffness of the beams and columns; the flexibility of the beam-column connections are often ignored although such flexibility may substantially increase deflections in a moment-resisting frame. Components of an SMF together with sample internal actions are shown in Figure. 9-2.

The AISC Seismic Provisions define three types of seismic steel moment-resisting frames: Ordinary Moment Frames, Intermediate Moment Frames, and Special Moment Frames. All three framing systems are designed assuming ductile behavior of varying degrees, for earthquake forces that are reduced from the elastic forces by a response modification factor, R (see Table 9-1 for values of R).

SMFs are considered to be the most ductile of the three types of moment frames considered by AISC. For this reason, and due to their architectural versatility, SMFs have been the most popular seismic framing system in high seismic regions in the United States. SMFs are designed for earthquake loads calculated using a value of R equal to 8. Stringent requirements are placed on the design of beams, columns, beam-to-column connections, and panel zones. Beam-to-column connections in SMFs are required to have a minimum inelastic rotation capacity of 0.03 radian.

Intermediate Moment Frames (IMFs) are assumed to be less ductile than SMFs but are expected to withstand moderate inelastic deformations in the design earthquake. IMFs are designed using a value of R equal to 6; fully restrained (FR) or partially restrained (PR) connections can be used in such frames. Beam-to-column connections in IMFs are required to have an inelastic rotation capacity of 0.02 radian. Other requirements are listed in the AISC Seismic Provisions (1997b).

Ordinary moment frames (OMFs) are less ductile than IMFs, and are expected to sustain only limited inelastic deformations in their components and connections in the design earthquake. Beam-to-column connections in OMFs are required to have an inelastic rotation capacity of 0.01 radian. FR and PR connections can be used in OMFs. Because OMFs are less ductile than IMFs, an OMF must be designed for higher seismic forces than an IMF; an OMF is designed for earthquake loads calculated using a value of R equal to 4.

The remainder of this section addresses issues associated with the design, detailing, and testing of special moment frames and components. The design philosophy for such frames is to dissipate earthquake-induced energy in plastic hinging zones that typically form in the beams and panel zones of the frame. Columns and beam-to-column connections are typically designed to remain elastic using capacity design procedures.

9.2.2 Analysis and Detailing of Special Moment Frames

Because the SMF is a flexible framing system, beam and column sizes in SMFs are often selected to satisfy story drift requirements. As such, the nominal structural strength of an SMF can substantially exceed the minimum base shear force required by the NEHRP Recommended Provisions. When analyzing SMFs, all sources of deformation should be considered in the mathematical model. NEHRP stipulates that panel zone deformations must be included in the calculation of story drift.

The AISC Seismic Provisions prescribe general requirements for materials and connections that are particularly relevant to SMF construction:

1. Steel in SMF construction must comply with the requirements described in Section 9.1.3. In addition, a minimum Charpy V-notch toughness of 20 ft-lbs at 70°F is required for thick materials in SMFs: ASTM A6 Group 3 shapes with flanges 1½ inches or thicker, ASTM A6 Groups 4 and 5 shapes, and plates that are 1½ inches or greater in thickness in built-up members.
2. Calculation of maximum component strengths (e.g., for strong column-weak beam calculations) for capacity design must be based on the expected yield strength, F_{ye} (see Eq. 9-6).
3. To prevent brittle fractures at the welds, AISC prescribes that welded joints be performed in accordance with an approved Welding Procedure Specifications and that all welds used in primary members and connections in the seismic force resisting system be made with a filler metal that has a minimum Charpy V-notch toughness of 20 ft-lbs at minus 20°F.

9.2.3 Beam Design

A beam in a steel SMF is assumed to be able to develop its full plastic moment (M_p) calculated as

$$M_p = Z_b F_y \qquad (9\text{-}7)$$

where Z_b is the plastic section modulus. In order to prevent premature beam flange or web local buckling, and to maintain this moment for large plastic deformations, the width-thickness ratios of the web and flange elements should be limited to the values of λ_{ps} given in Table 9-2. (The λ_p values are for non-seismic design.) In addition, both flanges of the beam must be laterally braced near potential plastic hinges; the unbraced length of the beam must not exceed $2500\, r_y / F_y$, where r_y is the radius of gyration about the weak axis for out-of-plane buckling.

9.2.4 Beam-to-Column Connections

Introduction

For discussion purposes, a beam-to-column connection includes the beam-column panel zone and the beam-to-column joints. Connections in an SMF need to satisfy three criteria: (1) a sufficient strength to develop the full plastic moment of the beam, (2) a sufficient stiffness to satisfy the assumption of a fully rigid (FR) connection, and (3) a large post-yield deformation capacity without significant loss of strength. Prior to the 1994 Northridge, California earthquake, the welded flange-bolted web steel moment connections were assumed by design professionals to easily satisfy all three criteria. Unfortunately, many moment-resisting connections suffered extensive damage during this earthquake. In addition to brittle fracture in the groove welded connections (mostly in the beam bottom flange), other types of fracture that were seldom observed in laboratory testing prior to the Northridge earthquake were also reported. Figure 9-3a shows cracks extending into the column panel zone, and Figure 9-3b presents a "divot" pullout from the column flange. The causes of failure are discussed in Bruneau et al. (1997).

The poor performance of welded moment-frame connections in more than 200 multistory buildings in the Northridge earthquake led to the development of a national program, funded by the Federal Emergency Management Agency (FEMA), to investigate the causes of failure and to develop alternative connections for repair, rehabilitation, and new construction. Part of the FEMA program involved full-scale testing of large-size steel beam-column connections (SAC 1996). The laboratory testing of the pre-Northridge prequalified welded flange-bolted web connection replicated many of the failure modes observed in the field after the earthquake. The mean value of beam plastic

Table 9-2. Limiting width-thickness ratios

Description of Element	Width-Thickness Ratio	λ_p	λ_{ps}
Flanges of I-shaped beams and channels in flexure	b/t	$65/\sqrt{F_y}$	$52/\sqrt{F_y}$
Webs of I-shaped beams in combined flexure and axial compression	h/t_w	for $P_u/\phi_b P_y \leq 0.125$: $\frac{640}{\sqrt{F_y}}\left(1-\frac{2.75P_u}{\phi_b P_y}\right)$ for $P_u/\phi_b P_y > 0.125$: $\frac{191}{\sqrt{F_y}}\left(2.33-\frac{P_u}{\phi_b P_y}\right) \geq \frac{253}{\sqrt{F_y}}$	for $P_u/\phi_b P_y \leq 0.125$: $\frac{520}{\sqrt{F_y}}\left(1-\frac{1.54P_u}{\phi_b P_y}\right)$ for $P_u/\phi_b P_y > 0.125$: $\frac{191}{\sqrt{F_y}}\left(2.33-\frac{P_u}{\phi_b P_y}\right) \geq \frac{253}{\sqrt{F_y}}$
Round HHS in axial compression or flexure	D/t	$\frac{2070}{F_y}$	$\frac{1300}{F_y}$
Rectangular HHS in axial compression or flexure	b/t	$\frac{190}{\sqrt{F_y}}$	$\frac{110}{\sqrt{F_y}}$

rotation capacity from all of the tests of the pre-Northridge connection detail was 0.004 radian (Whittaker et al. 1998), which was significantly less than the target value of 0.03 radian. In response to these findings, the 1997 AISC Seismic Provisions require that (1) the design of beam-to-column joints and connections in SMFs must be based on qualifying tests of at least two specimens, and (2) each connection must develop a plastic rotation of 0.03 radian.

Beam-to-Column Connection Details

Shortly after the 1994 earthquake, the prequalified welded flange-bolted web connection was deleted from most building codes and replaced by general provisions that required the design professional to demonstrate the adequacy of the connection by either full-scale testing or calculations supported by test data. In response to this action, design professionals have proposed new types of moment-resisting connections for steel buildings. Some of these proposals are discussed below. In all cases, the proposed connection details relocate the beam plastic hinge away from the face of the column. Only welded connections are considered in this section.

These connection details fall in one of the two categories: weakening the beam cross-section away from the face of the column, or reinforcing the beam cross-section at the column face. Only non-proprietary moment connections are discussed.

Reinforced Connections

A variety of reinforced connections have been developed since the Northridge earthquake. Some reinforced connection details are shown in Figure. *9*-4: cover plates, welded flange plates, triangular haunches, straight haunches, and vertical plate ribs. Note that these connection details would not only increase the beam plastic hinge rotation demand but also increase the maximum moment demand at the face of the column, which could require a stronger panel zone or a larger section for the column to maintain the strong column-weak beam system (SAC 1995). Typical design practice for reinforced connections is to keep the reinforced component in the elastic range for moments associated with substantial strain

hardening in the beam beyond the reinforcement. Although it may be tempting to assume a linear distribution of bending moment along the length of the beam to size the reinforcement, the effects of gravity load on the beam bending moment diagram, if significant, must be carefully considered. For all of the connection details described below, notch-toughness rated weld filler metal, qualified welders, and high quality inspection should be specified.

Immediately after the Northridge earthquake, cover plates (see Figure 9-4a) have been one of the more popular strategies for reinforcing beam-to-column connections. Testing has been completed at a number of laboratories and significant data are available (e.g., Engelhardt and Sabol 1996, and SAC 1996). In most cases, the bottom cover plate is rectangular and wider than the beam bottom flange, and the top cover plate is tapered and narrower than the beam top flange. This configuration permits the bottom cover plate to be used as an erection seat, and facilitates down-hand welding in the field. Welded, not bolted, web connections are recommended as an effective way of reducing the thickness of the cover plates. Although a significant number of cover plated connection specimens have achieved beam plastic rotations exceeding 0.03 radian, Hamburger (1996) reported a failure rate of approximately 20 percent for cover-plated connections in laboratory tests. Another concern with the cover-plate connection is that the seam between the flange cover plate and the beam flange acts as a notch at the column face that may lead to cracks propagating into the column flange and beyond. Further information is available in SAC (1997).

The welded flange-plate connection (see Figure 9-4b) is closely related to the cover-plate connection, with the major difference being that only the flange plates are groove welded to the column (Jokerst and Soyer 1996, Noel and Uang 1996). As such, flange plates of the welded flange-plate connection are thicker than the comparable cover plates shown in Figure 9-4a. There is no notch effect associated with the welded flange-plate connection because the beam flanges are not welded to the column flange. The bottom welded flange plate can be shop welded to the column, thereby eliminating one field groove weld, and providing an erection seat for the beam.

Welded triangular and straight haunch reinforced connections (see Figures 9-4c and d) underwent extensive laboratory testing following the Northridge earthquake (e.g., SAC 1996, Gross et al. 1998) because both reinforcements could be used for seismic repair and retrofit. Most of the haunch connection tests conducted to date incorporated a haunch to the bottom flange, although the addition of haunches to both the top and bottom flanges was also considered. Of the different types of haunch details tested to date, the triangular T-shaped haunches appear to be the most effective (Yu et al. 2000). Large plastic rotations were achieved with this type of connection. Vertical rib plates (see Figure 9-4e) can also be used to reduce the stress demand in the welded joint (Chi and Uang 2000).

Reduced Beam Sections

An alternative to relocating the plastic hinge away from the face of the column is to reduce the plastic moment of the beam at a short distance from the column face. Beam sections can be reduced by tapering the flanges, or by radius-cutting the flanges as shown in Figure 9-5. The latter approach appears to be the most promising because the re-entrant corners of the tapered flange profile tend to promote pre-mature fracture in the beam flanges.

Originally proposed and tested by Plumier (1990), the use of the reduced beam section (RBS), also termed the *dogbone* by many design professionals, has seen broad support from engineers, steel producers, and fabricators. Both reduced-beam-section profiles have achieved plastic rotations in excess of 0.03 radian. Additional information is provided in Iwankiw and Carter (1996), Chen et al. (1996), Engelhardt et al. (1996), and Zekioglu et al. (1996).

(a) Beam bottom flange weld fracture propagating through column flange and web

(b) Beam bottom flange weld fracture causing a column divot fracture

Figure 9-3. Examples of brittle fracture of steel moment frame connections (courtesy of David P. O'sullivan, EQE International, San Francisco)

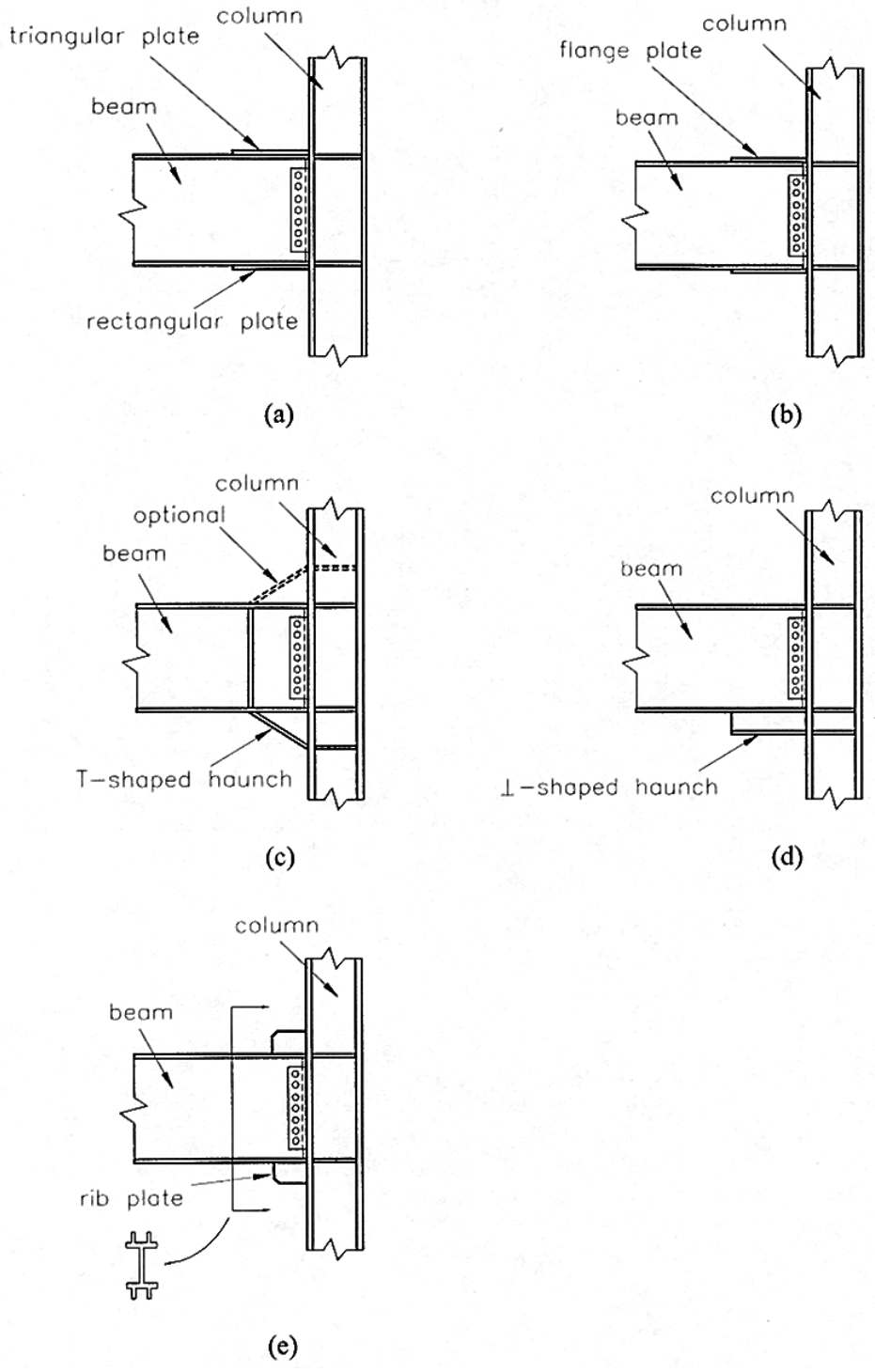

Figure 9-4. Reinforced moment connections: (a) cover plates, (b) welded flange plates, (c) triangular haunches, (d) straight haunch, (e) rib plates

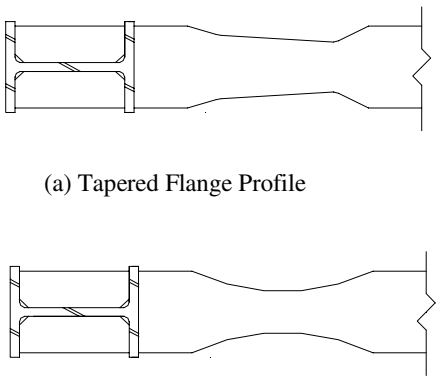

(a) Tapered Flange Profile

(b) Circular Flange Profile

Figure 9-5. Moment connection with reduced beam section

Reducing the width of the beam flange serves to delay flange local buckling but increases the likelihood of web local buckling and lateral-torsional buckling because the in-plane stiffness of the flanges is significantly reduced. The reduced beam section usually experiences web local buckling first, followed by lateral-torsional buckling and flange local buckling.

The stability of RBS beams was studied as part of the SAC Joint Venture (Uang and Fan 2000). It was found from a statistical study that web local buckling is the governing mode of buckling. While the λ_{ps} values presented in Section 9.2.3 for flange local buckling and lateral-torsional buckling still can be used for RBS design, the λ_{ps} value for web local buckling needs to be reduced from $520/\sqrt{F_y}$ to $418/\sqrt{F_y}$ (SAC 2000). The study also showed that additional lateral bracing near the RBS is generally unnecessary.

Design engineers frequently use deep columns in a moment frame to control drift. When the deep section wide-flange columns are used, however, an experimental study showed that significant torsion leading to the twisting of the column could result (Gilton et al. 2000). Two factors contribute to the column twisting. First, the lateral-torsional buckling amplitude of the beam tends to be larger when the RBS is used. Second, the stress in the column produced by warping torsion is highly dependent on the ratio $(d_c - t_{cf})/t_{cf}^3$. For example, this ratio is equal to 0.671/in^2 for a W14×398 section (I_x = 6000 in^4). If the designer chooses a deep section W27×161 for a comparable moment of inertia (I_x = 6280 in^4) to control drift, the ratio is drastically increased to 21.04/in^2, implying that this section is susceptible to column twisting. Lateral bracing near the RBS region then may be required to minimize the twisting. A procedure to check if column twisting is a concern has been developed (Gilton et al. 2000).

9.2.5 Beam-to- Column Panel Zones

Introduction

A beam-to-column panel zone is a flexible component of a steel moment-resisting frame that is geometrically defined by the flanges of the column and the beam (see Figure 9-6).

Although seismic building codes require the consideration of panel zone deformations in the story drift computations, panel zones are rarely modelled explicitly in mathematical models of steel moment-resisting frames. Mathematical representations of moment-resisting frames are generally composed of beams and columns modelled as line elements spanning between the beam-column intersection points. Such a representation will underestimate the elastic flexibility of a moment-resisting frame. An approximate analysis procedure that includes the flexibility of panel zones for drift computations have been proposed (Tsai and Popov 1990). This procedure will be demonstrated in an SMF design in Section 9.5.2.

Typical internal forces on a panel zone are shown in Figure 9-6a; axial, shearing, and flexural forces are typically present in a panel zone. In this figure, continuity plates are shown in the column at the level of the beam flanges and the moments M_1 and M_2 represent

earthquake actions. Assuming that the flanges resist 100 percent of the moment and that the distance between the centroids of the flanges is 95 percent of the beam depth, compression and tension flange forces as shown in Figure 9-6b can replace the beam moments.

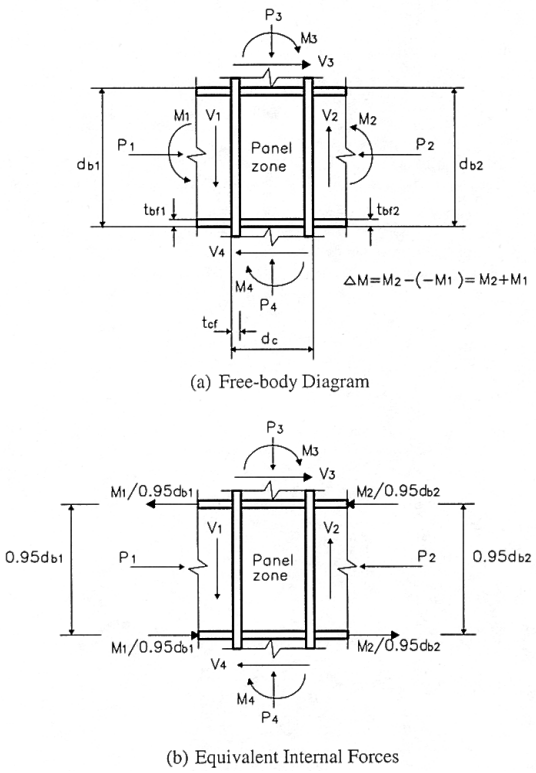

Figure 9-6. Internal forces acting on a panel zone of a moment-resisting frame subjected to lateral loading

The continuity plates shown in Figure 9-6 serve to prevent column flange distortion and column web yielding and crippling. If such plates are not provided in a column with thin flanges, and the beam flange imposes a tensile force on the column flange, inelastic strains across the groove weld of the beam flange are much higher opposite the column web than they are at the flange tips. Thus, weld cracks and fractures may result. Because the design of beam-to-column joints and connections is based upon qualifying cyclic tests, AISC (1997) requires that continuity plates of the size used in the qualifying tests be provided in the connection. However, welding of the highly restrained joints, such as continuity plates, induces residual stress in steel members. In addition to the normal variation of material properties in the column, the process of mill rotary straightening of the W-shaped member alters the mechanical properties by cold working in the "k" area. (The "k" area is defined by AISC as the region extending from about the midpoint of the radius of the fillet into the web approximately 1 to 1.5 in. beyond the point of tangency between the fillet and web.) As a result, a reduction in ductility and toughness in the "k" area may occur. In some cases, values of Charpy V-notch toughness less than 5 ft-lb at 70° F have been reported. Since welding in the "k" area may increase the likelihood of fracture, a recent AISC Advisory (1997a) has suggested that welds for the continuity plates be stopped short of the "k" area. Fillet welds and/or partial joint penetration welds, proportioned to transfer the calculated forces, are preferred to complete joint penetration welds.

Required Shear Strength

Using the information presented in Figure 9-6b, and taking a free-body diagram immediately below the upper continuity plate, the horizontal shearing force in the panel zone (V_{pz}) can be calculated as

$$V_{pz} = \frac{M_1}{0.95d_{b1}} + \frac{M_2}{0.95d_{b2}} - V_c \qquad (9\text{-}8)$$

where all terms are defined above and in the figure, and V_c is the shearing force in the column immediately above the panel zone. Because V_c reduces the shearing force in the panel zone, and its magnitude is substantially smaller than the first two terms on the right hand side of this equation, V_c can be ignored conservatively in the calculation of the maximum shearing force. Therefore, for beams of equal depth,

$$V_{pz} \approx \frac{\Delta M}{d_b} \qquad (9\text{-}9)$$

where $\Delta M = (M_1 + M_2)$ is the unbalanced beam moment.

Prior to the publication of the 1988 Uniform Building Code (ICBO 1988), panel zones were designed to remain elastic for $M_1 = M_2 = M_p$, where M_p is the nominal plastic moment of the beam under consideration. The strength of the panel zone at first yield was computed as $0.55F_{yc}A_{wc}$, where F_{yc} is the nominal yield strength of the column and A_{wc} is the area of the column web $(= d_c t_{cw})$. This design procedure was intended to produce *strong panel zones* such that yielding in the moment-resisting frame was minimized in the panel zone region.

Both the 1988 Uniform Building Code and the 1992 AISC Seismic Provisions relaxed the design provisions for panel zone regions and permitted *intermediate strength panel zones* and *minimum strength panel zones*. Previous studies by Krawinkler et al. (1975) had shown that panel zone yielding could dissipate a large amount of energy in a stable manner. Intermediate and minimum strength panel zones were introduced to encourage panel zone yielding. According to the 1992 AISC Seismic Provisions, intermediate strength panel zones were designed for

$$\Delta M = \sum M_p - 2M_g \qquad (9\text{-}10)$$

where M_g is the gravity moment for one beam. If the gravity moment is taken to be 20 percent of the plastic moment, the above equation gives $\Delta M = 0.8\Sigma M_p$. Minimum strength panel zones were allowed for a value of $\Delta M = \Sigma M_E \le 0.8\Sigma M_p$, where the unbalanced beam moment produced by the prescribed design seismic forces is $\Sigma M_E = (M_{E1} + M_{E2})$. It has been shown (Tsai and Popov 1988) that steel moment frames with intermediate- or minimum-strength panel zones are likely to have a substantially smaller overstrength factor, Ω_o, than those with strong panel zones. In addition, the lateral stiffness of an intermediate- or minimum-strength panel-zone frame can be significantly smaller than that computed using a mathematical model based on centerline dimensions.

Current AISC provisions (AISC 1997) require the use of Ω_o equal to 3.0 (see Table 9-1) for beam moments induced by the design earthquake loads. It also replaces the nominal plastic moment by the expected plastic moment and prescribes that the required strength of a panel zone need not exceed the shear force determined from $0.8\sum M^*_{pb}$, where $\sum M^*_{pb}$ is the sum of the beam moment(s) at the intersection of the beam and column centrelines. ($\sum M^*_{pb}$ is determined by summing the projections of the expected beam flexural strength(s) at the plastic hinge location(s) to the column centreline.) That is, the panel zone shall be designed for the following unbalanced moment:

$$\Delta M = \Omega_o \Sigma M_E \le 0.8\Sigma M^*_{pb} \qquad (9\text{-}11)$$

Substituting Eq. (9-11) into Eq. (9-9) would give the required shear strength in the panel zone.

Post-Yield Strength and Detailing Requirements

The 1992 AISC equation for calculating the design shear strength of a panel zone ($\phi_v V_n$, where ϕ_v=0.75) was based on the work of Krawinkler et al. (1975):

$$\phi_v V_n = \phi_v \left[0.60 F_{yc} d_c t_p \left(1 + \frac{3 b_{cf} t_{cf}^2}{d_b d_c t_p} \right) \right] \qquad (9\text{-}12)$$

where d_c is the depth of the column, t_p is the total thickness of the panel zone, including doubler plates ($t_p = t_{cw}$ if no doubler plates are present), b_{cf} is the width of the column flange, t_{cf} is the thickness of the column flange, and d_c is the depth of the column. The second term

in the parentheses represents the contribution of column flanges (assumed to be linearly elastic) to the shear strength of the panel zone. The equation used to calculate V_n assumes a level of shear strain of $4\gamma_y$ in the panel zone, where γ_y is the yield shearing strain.

A panel zone must also be checked for a minimum thickness (t) to prevent premature local buckling under large inelastic shear deformations:

$$t = \frac{(d_z + w_z)}{90} \qquad (9\text{-}13)$$

In this empirical equation, d_z is the depth of the panel zone between the continuity plates, and w_z is the width of the panel zone between the column flanges. If doubler plates are used to satisfy this equation for t, the plates must be plug welded to the column web such that the plates do not buckle independently of the web.

If used, doubler plates must be welded to the column flanges using either a complete joint penetration groove weld or a fillet weld that develops the design shear strength of the full doubler plate thickness. When such plates are welded directly to the column web and extend beyond the panel zone, minimum weld size can be used to connect the top and bottom edges to the column web. However, because of the cold working due to the rotary straightening practice and the resulting variations of material properties exhibited in the column "k" areas, the AISC Advisory (1997) suggested that, as an interim measure, the design engineer increase the column size to avoid the use of doubler plates.

9.2.6 Column Design

The column of an SMF must be designed per the LRFD Specifications (1997) as a beam-column to avoid axial yielding, buckling, and flexural yielding. Columns are routinely spliced by groove welding. Such connections are required to have sufficient strength to resist the imposed axial, shearing, and flexural forces calculated using the specified load combinations. In addition, the column axial strength should be sufficient to resist the axial forces produced by the special load combinations of Eqs. 9-4 and 9-5. Additional strength is required if either the welds are partial penetration groove welds or the welds are subjected to net tension forces. Column splices using fillet welds or partial joint penetration groove welds shall not be located within 4 feet or one-half the column clear height of beam-to-column connections, which is less.

Special moment frames are designed using the strong column-weak beam philosophy because such an approach improves the energy dissipation capacity of the frame, promotes plastic hinge formation in the beams, increases the seismic resistance of the frame, and ostensibly prevents the formation of a soft story mechanism. Seismic regulations seek to achieve a strong column-weak beam system by ensuring that, at a beam-to-column connection, the sum of the column plastic moments exceeds the sum of the beam plastic moments. With few exceptions, AISC (1997) requires that:

$$\frac{\sum M^*_{pc}}{\sum M^*_{pb}} > 1.0 \qquad (9\text{-}14)$$

where $\sum M^*_{pc}$ is the sum of the moment capacities in the columns above and below the joint at the intersection of the beam and column centerlines, and $\sum M^*_{pb}$ is the sum of the moment demands in the beams at the intersection of the beam and column centerlines.

The value of $\sum M^*_{pc}$ is determined by summing the projections of the *nominal* flexural strength of the columns above and below the connection to the beam centerline, with a reduction for the axial force in the column. ΣM^*_{pc} can be conservatively approximated as $\sum Z_c (F_{yc} - P_{uc} / A_g)$, where A_g is the gross area of the column, P_{uc} is the required column compressive strength, Z_c is the

plastic section modulus of the column, and F_{yc} is the minimum specified yield strength of column. The value of $\sum M_{pb}^{*}$ is calculated by summing the projection of the expected beam flexural strengths at the plastic hinge locations to the column. $\sum M_{pb}^{*}$ can be approximated as $\sum(1.1R_yF_yZ + M_v)$, where Z is the plastic modulus of the beam section at the potential plastic hinge location, and M_v accounts for the additional moment due to shear amplification from the location of the plastic hinge to the column centerline. As illustrated in Figure 9-7, for reinforced connections using haunches or vertical ribs, SAC (1996) suggests that plastic hinges be assumed to be located at a distance s_h = d/3 from the toe of haunch or ribs. For cover plated connections, SAC recommends that the plastic hinge be located at a distance s_h = d/4 beyond the end of cover plate. When the ratio in Eq. 9-14 is no greater than 1.25, the width-to-thickness ratios of the flange and web elements of the column section shall be limited to the λ_{ps} values in Table 9-2 because plastic hinge formation in the column may occur due to the shift of inflection point during an earthquake. Otherwise, columns shall comply with the limiting values of λ_p in the same table.

9.3 Behavior and Design of Concentrically Braced Frames

9.3.1 Design Philosophy

Concentrically braced frames are frequently used to provide lateral strength and stiffness to low- and mid-rise buildings to resist wind and earthquake forces. Although some architects favor the less intrusive moment frames, others have found architectural expression in exposing braced frames which the public intuitively

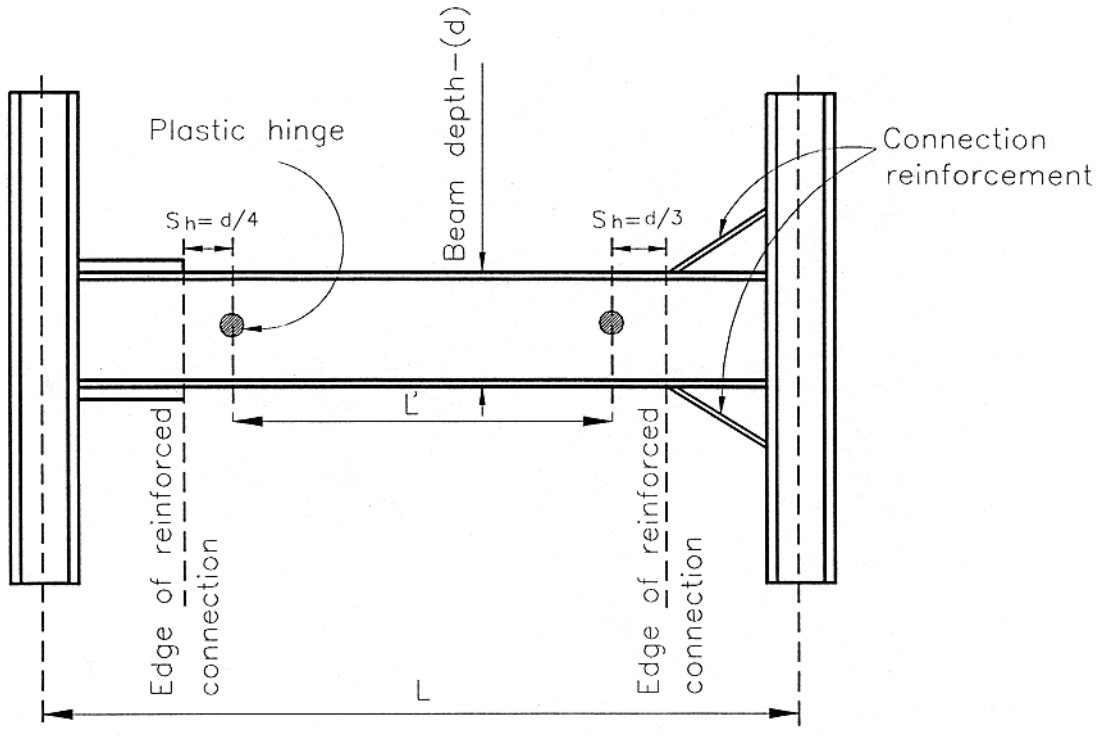

Figure 9-7. Assumed beam plastic hinge locations (Adapted from Interim Guidelines Advisory No. 1, SAC 1997)

associates with seismic safety in some earthquake-prone regions. However, for those frames to provide adequate earthquake resistance, they must be designed for appropriate strength and ductility. This is possible for many of the concentrically braced frame (CBF) configurations shown in Figure 9-8, but not all, as described in this section.

In a manner consistent with the earthquake-resistant design philosophy presented elsewhere in this chapter, modern concentrically braced frames are expected to undergo inelastic response during infrequent, yet large earthquakes. Specially designed diagonal braces in these frames can sustain plastic deformations and dissipate hysteretic energy in a stable manner through successive cycles of buckling in compression and yielding in tension. The preferred design strategy is, therefore, to ensure that plastic deformations only occur in the braces, leaving the columns, beams, and connections undamaged, thus allowing the structure to survive strong earthquakes without losing gravity-load resistance.

Past earthquakes have demonstrated that this idealized behavior may not be realized if the braced frame and its connections are not properly designed. Numerous examples of poor seismic performance have been reported (Tremblay et al. 1995, 1996; AIJ 1995). As shown in Figure 9-9, braces with bolted connections have fractured through their net section at bolt holes, beams and columns have suffered damage, and welded and bolted connections have fractured. Collapses have occurred as a consequence of such uncontrolled inelastic behavior.

The design requirements necessary to achieve adequate strength and ductility in concentrically braced frames are presented in this section. Two types of systems are permitted by the AISC Seismic Provisions: Special

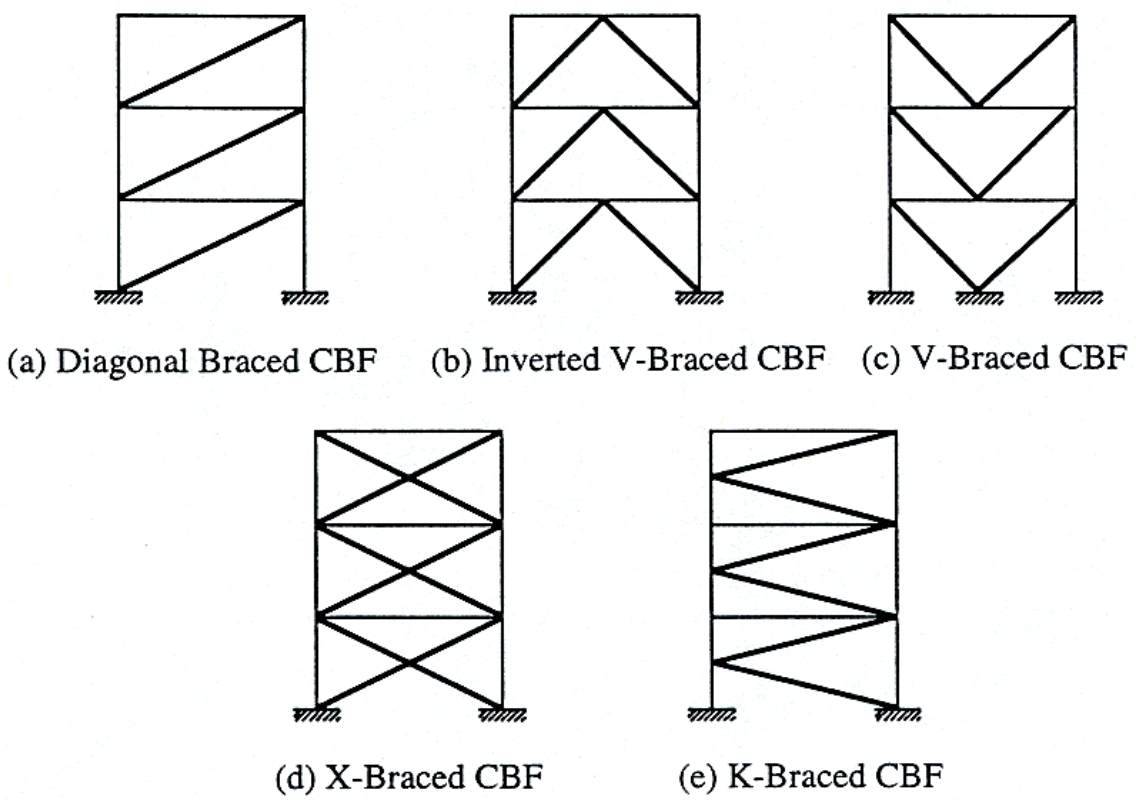

Figure 9-8. Typical brace configuration

Concentrically Braced Frames (SCBs) and Ordinary Concentrically Braced Frames (OCBFs). The emphasis herein is on the SCBF, which is designed for stable inelastic performance using a response modification factor, *R*, of 6. Some of the more stringent ductile detailing requirements are relaxed for the OCBFs because it is assumed that these frames will be subjected to smaller inelastic deformation demands due to the use of a smaller response modification factor. However, if an earthquake greater than that considered for design occurs, SCBFs are expected to perform better than OCBFs because of their substantially improved deformation capacity.

9.3.2 Hysteretic Energy Dissipation Capacity of Braces

Given that diagonal braces are the structural members chosen to plastically dissipate seismic energy, an examination of the physical behavior of a single brace subjected to axial load reversal is useful. It is customary to express the inelastic behavior of axially loaded members in terms of the axial force, *P*, versus the axial elongation, δ. According to convention, tension forces and elongations are expressed with positive values. A schematic representation of such a hysteretic curve is shown in Figure 9-10. Note that the transverse member deflection at mid-span is represented by Δ.

A full cycle of inelastic deformations can be described as follows. Starting from an initially unloaded condition (point O in Figure 9-10), the member is first compressed axially in an elastic manner. Buckling occurs at point A. Slender members will experience elastic buckling along plateau AB, for which the applied axial force can be sustained while the member deflects laterally. Up to that point, the brace behavior has remained elastic and unloading would proceed along the line BAO if the axial compressive was removed.

During buckling, flexural moments develop along the member, equal to the product of the axial force and lateral deflection, with the largest value reached at the point of maximum deflection, Δ, at mid-span. Eventually, the plastic moment of the member, reduced by the axial load, is reached at mid-span, and a plastic hinge starts to develop there (point B in Figure 9-10). The interaction of flexure and axial force on the plastic moment must be taken into account to determine the actual value of Δ corresponding to point B. Along segment BC, further increases in Δ result in greater plastic hinge rotations at mid-span (i.e., the member develops a "plastic kink") and a corresponding drop in axial resistance. The relationship between *P* and δ is nonlinear, partly as a result of the plastic interaction between flexure and axial force.

Upon unloading (starting at point C in Figure 9-10), the applied compression force is removed in an elastic manner. After unloading, the member retains a large residual axial deformation as well as a large lateral deflection. When loading the member in tension, behavior is first elastic, up to point D. Then, at point D, the product of the axial force, *P*, and the mid-span transverse deformation, Δ, equals the member reduced plastic moment and a plastic hinge forms at mid-span. However, this time, along segment DE, plastic hinge rotations act in the reverse sense to those along segment BC, and the transverse deflection reduces. As a result, progressively larger axial forces can be applied. The bracing member cannot be brought back to a perfectly straight position before the member yields in tension. Consequently, when unloaded and reloaded in compression, the brace behaves as a member with an initial deformation and its buckling capacity, P'_{cr}, is typically lower that the corresponding buckling capacity upon first loading, P_{cr}. Upon further cycles of loading, the value of P'_{cr} rapidly stabilizes to a relatively constant value. Typically, the ratio of P'_{cr}/P_{cr} depends on the member slenderness ratio, *KL/r*, and expressions have been proposed to capture this relationship (Bruneau et al. 1997). For simplicity, a constant value of $P'_{cr} = 0.8P_{cr}$ is specified in the AISC Seismic Provisions (1992) and must be considered whenever it gives a more critical design condition.

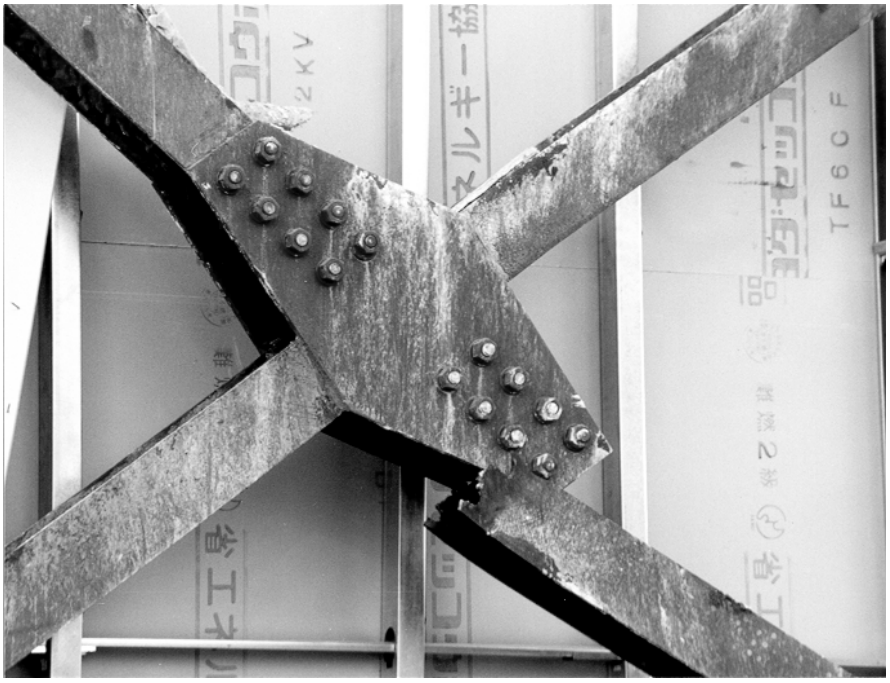

(a) Net section fracture at bolt holes

(b) Severe distortion of beam without lateral support at location of chevron braces

Figure 9-9. Examples of damage to non-ductile braced frames

(c) Fracture of welded connection and web tear-out in brace

(d) Weld fracture

Figure 9-9 Examples of damage to Non-Ductile braced frames (continued)

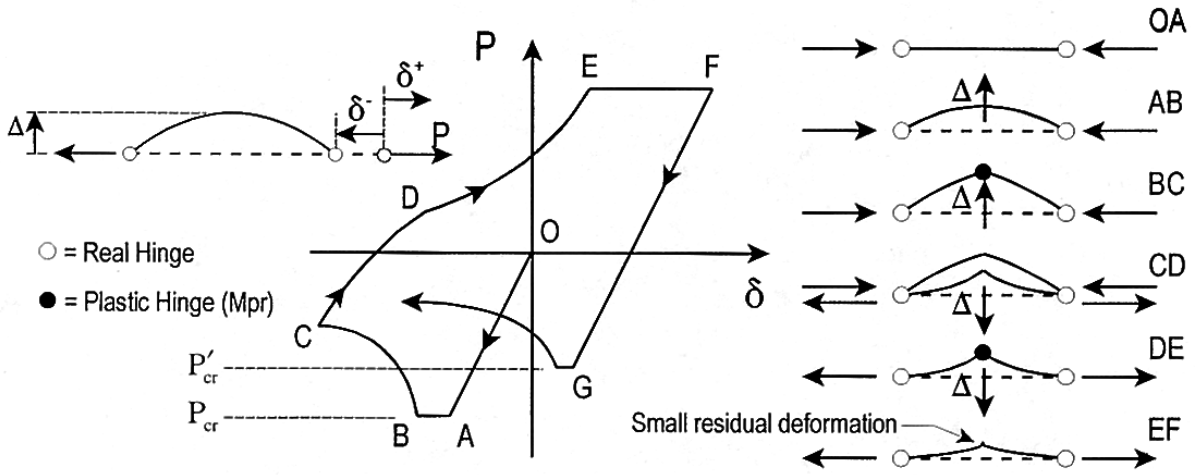

Figure 9-10. Hysteresis of a brace under cyclic axial loading

Beyond this difference, the hysteretic curve repeats itself in each subsequent cycle of axial loading and inelastic deformations, with a shape similar to the OABCDEF of Figure 9-10.

9.3.3 Design Requirements

Concentrically braced frames exhibit their best seismic performance when both yielding in tension and inelastic buckling in compression of their diagonal members contribute significantly to the total hysteretic energy dissipation. The energy absorption capability of a brace in compression depends on its slenderness ratio (*KL/r*) and its resistance to local buckling during repeated cycles of inelastic deformation.

Limits on Effective Slenderness Ratio

As can be deduced from Figure 9-10, slenderness has a major impact on the ability of a brace to dissipate hysteretic energy. For a very slender brace, segment OA is short while

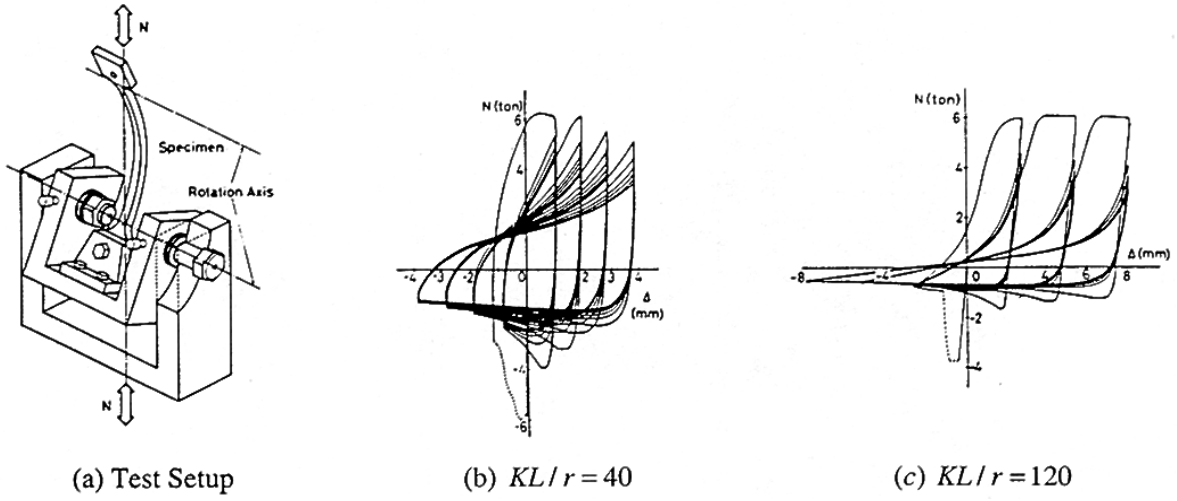

Figure 9-11. Brace Hysteresis loops by experimentation. (Nakashima and Wakabayashi 1992, referring to a figure by Shibata et al. 1973, with permission from CRC Press, Boca Raton, Florida)

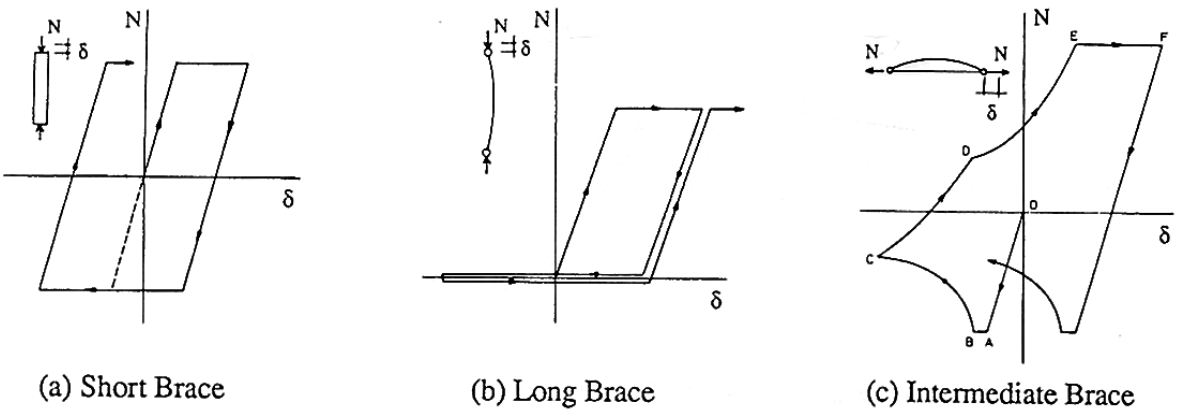

Figure 9-12. Schematic hysteretic behavior of braces of short, long, and intermediate slenderness (Nakashima and Wakabayashi 1992, with permission from CRC Press, Boca Raton, Florida).

segment AB is long, resulting in poor energy dissipation capacity in compression. For stocky braces, the reverse is true, and segment AB (i.e., elastic buckling) may not exist. Slenderness has no impact on the energy dissipation capability of braces in tension.

Typical hysteretic loops obtained experimentally for axially loaded members of intermediate and large slenderness ratios are shown in Figure 9-11, where the parameter λ ($=Kl/(r\pi)\sqrt{F_y/E}$) is a non-dimensional slenderness ratio (Nakashima and Wakabayashi 1992). Schematic illustrations of simplified hysteresis loops for short, intermediate and long braces are shown in Figure 9-12.

Very slender brace members (such as bars or plates) can result from a practice called tension-only design, often used prior to the promulgation of modern seismic provisions for steel buildings, and still used in non-seismic regions. In that design approach, the tension brace is sized to resist all the lateral loads, and the contribution of the buckled compression brace is ignored. While tension-only design may be acceptable for wind resistance, it is not permissible for earthquake resistance. As shown in Figure 9-13, braced frames with very slender members must progressively drift further and further to be able to dissipate the same amount of energy at each cycle, perhaps leading to collapse due to second-order effects.

Seismic detailing provisions typically limit brace slenderness to prevent the above problem and to ensure good energy dissipation capacity. Many seismic codes require:

$$\frac{KL}{r} \le \frac{720}{\sqrt{F_y}} \qquad (9\text{-}15)$$

where F_y is in ksi. For ASTM A992 or A572 Grade 50 steel, this corresponds to an effective slenderness ratio of 102. Recently, the AISC Seismic Provisions (1997) have relaxed this limit to:

$$\frac{KL}{r} \le \frac{1000}{\sqrt{F_y}} \qquad (9\text{-}16)$$

for bracing members in SCBFs, but kept the more stringent limit of Eq. 9-15 for OCBFs. Nevertheless, the authors recommend the use of Eq. 9-15 for both SCBFs and OCBFs.

Limits on Width-to-Thickness Ratio

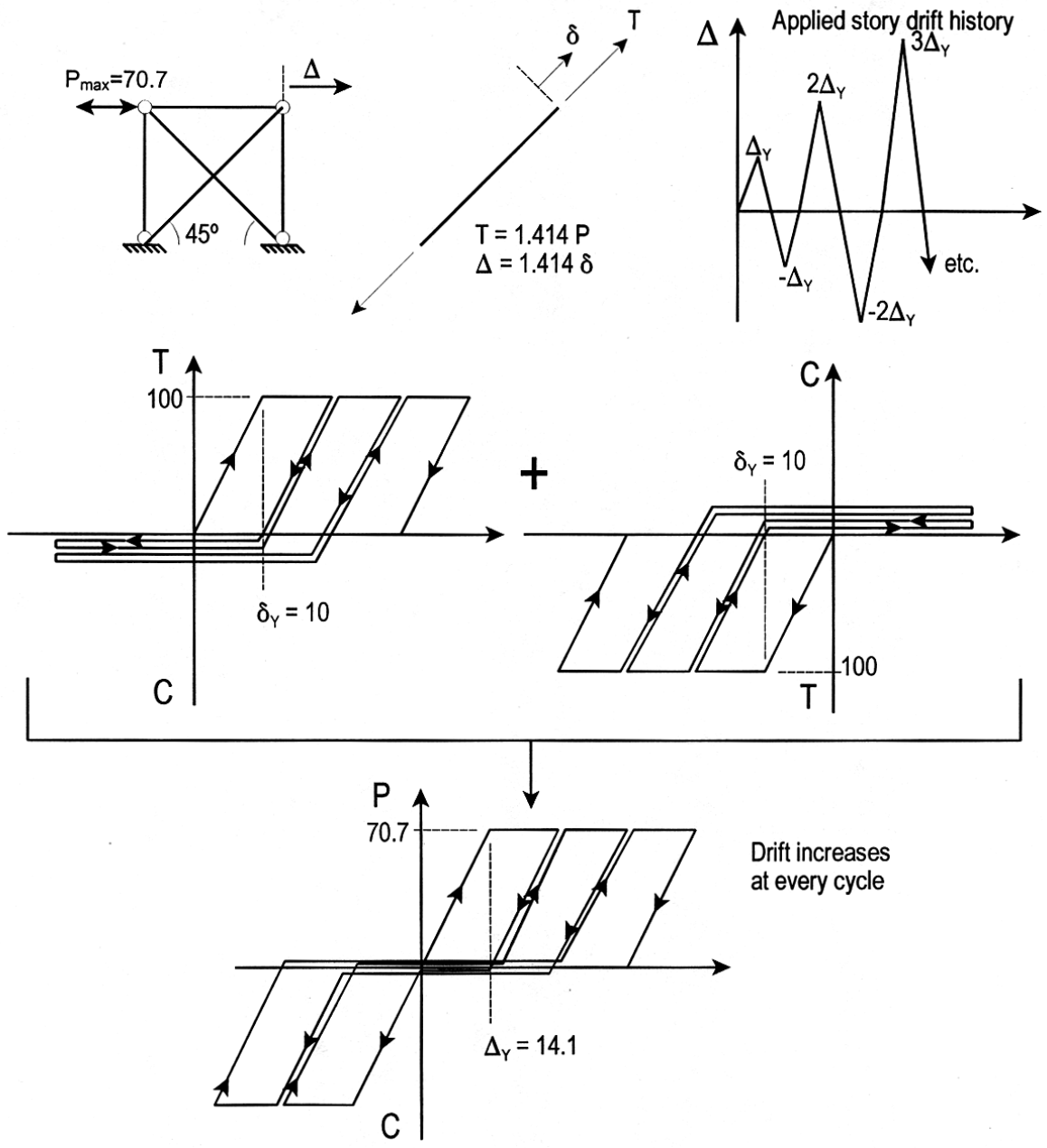

Figure 9-13. Hysteretic Behavior of Single-Story braced frame having very slender braces

The plastic hinge that forms at mid-span of a buckled brace may develop large plastic rotations that could lead to local buckling and rapid loss of compressive capacity and energy dissipation during repeated cycles of inelastic deformations. Past earthquakes and tests have shown that locally buckled braces can also suffer low-cycle fatigue and fracture after a few cycles of severe inelastic deformations (especially when braces are cold-formed rectangular hollow sections). For these reasons, braces in SCBFs must satisfy the width-to-thickness ratio limits for compact sections. For OCBFs, braces can be compact or non-

compact, but not slender, i.e., $b/t \leq \lambda_r$ per LRFD Specification. Based on experimental evidence, more stringent limits are specified for some types of structural shapes. In particular, the width-to-thickness ratio of angles (*b/t*), the outside diameter to wall thickness ratio of unstiffened circular hollow sections (*D/t*), and the outside width to wall thickness ratio of unstiffened rectangular sections must not exceed $52/\sqrt{F_y}$, $1300/F_y$, and $110/\sqrt{F_y}$, respectively (see Table 9-2). Note that the AISC Seismic Provisions (1997) define *b* for rectangular hollow sections as the "out-to-out width", not the flat-width (= $b-3t$) as defined in the AISC Specifications (AISC 1994).

Redundancy

Energy dissipation by tension yielding of braces is more reliable than buckling of braces in compression. To provide structural redundancy and a good balance of energy dissipation between compression and tension members, structural configurations that depend predominantly on the compression resistance of braces should be avoided. Examples of poor braced frames layout are shown in Figure 9-14, together with recommended alternatives. Four braces in compression and only one brace in tension resist the load applied on the 5-bay braced frame shown in Figure 9-14a. All braces in the braced-core of Figure 9-14c are in compression to resist the torsional moment resulting from seismically-induced inertial force acting at the center of mass. (For simplicity, columns resisting only gravity loads are not shown in that figure.) Better designs are shown in Figures 9-14b and 9-14d for each of these cases, respectively.

Seismic design codes attempt to prevent the use of non-redundant structural systems by requiring that braces in a given line be deployed such that at least 30% of the total lateral horizontal force acting along that line is resisted by tension braces, and at least 30% by compression braces. Although the wording of such clauses does not cover the case shown in Figure 9-14c, the intent does. Codes generally waive this requirement if nearly elastic response is expected during earthquakes, something achieved in the AISC Seismic Provisions by the special load conditions described in Section 9.1. Note that in calculating the strength of an OCBF, the AISC Seismic Provisions also require that $\phi_c P_{cr}$ (= $0.9\phi_c P_{cr}$) be used instead of $\phi_c P_{cr}$, for the reasons described in the previous section. There is no such requirement for SCBFs, but the authors prefer to observe this requirement for both OCBFs and SCBFs, recognizing, however, that the tension brace may have sufficient strength to accommodate the strength degradation of the compression brace upon repeated cycling, and that such a force redistribution may be considered when calculating the strength of the braced panel using $\phi_c P_{cr}$. This approach is not recommended for V- and inverted-V-types of OCBF.

9.3.4 Bracing Connections Design Requirements

When a brace is in tension, net section fracture and block shear rupture at the end of the brace must be avoided. Likewise, the brace connections to beams and columns must be stronger than the braces themselves. Using capacity design, calculation of brace strength must recognize that the expected yield strength of the brace, F_{ye}, will typically exceed its specified minimum yield strength, F_y (see Eq. 9-6). Thus, connections must be designed to resist an axial force equal to $R_y F_y A_g$. However, when plastic analysis is used to demonstrate that braces are unlikely to yield, connections may be designed for the maximum force obtained from such an analysis.

Connections must also be able to resist the forces due to buckling of the brace. If strong connections permit the development of a plastic hinge at each end of a brace, they should be designed to resist a moment equal to $1.1R_y M_p$ of the brace in the direction of buckling. Otherwise, the connecting elements will themselves yield in flexure (such as gussets out

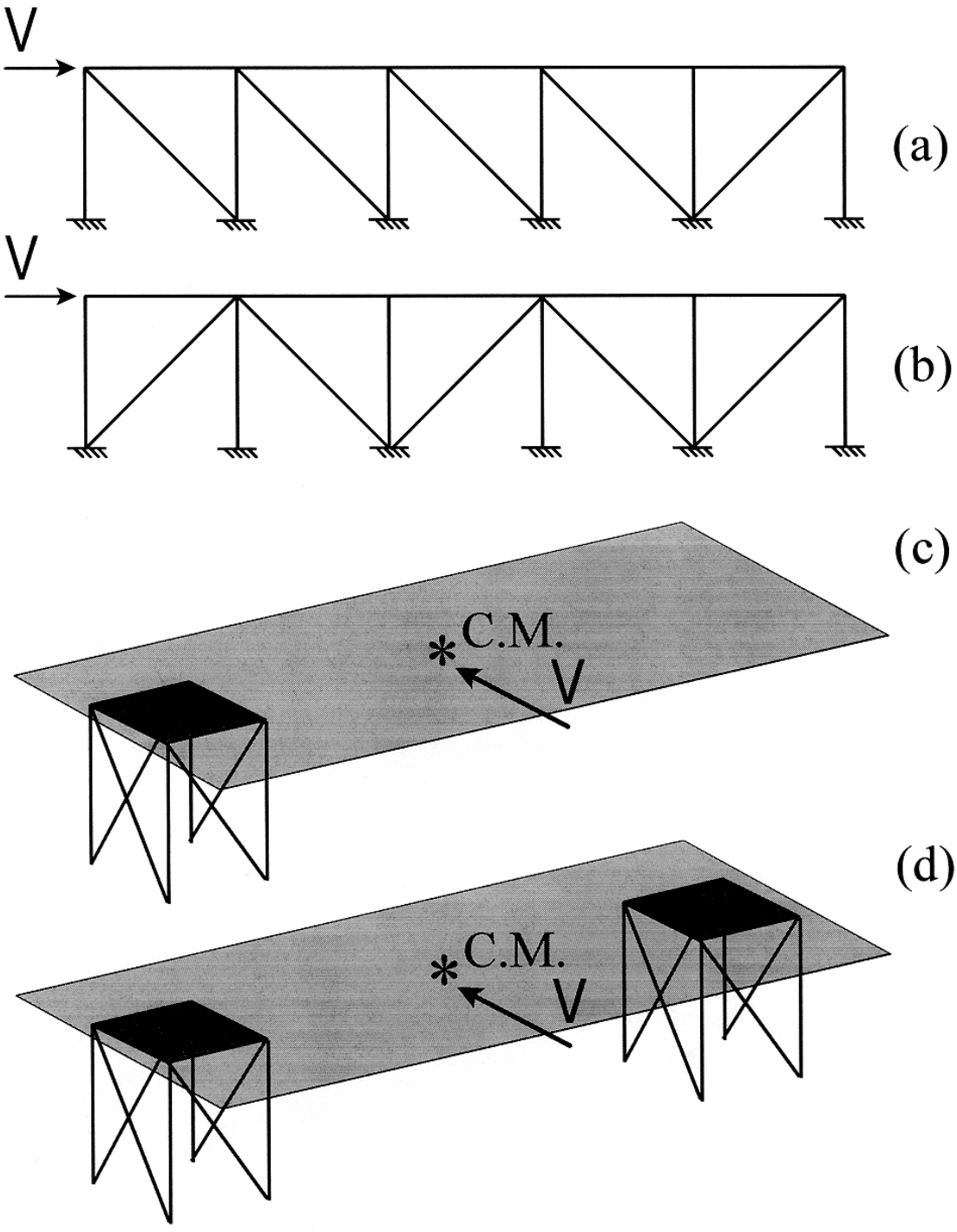

Figure 9-14. Brace configurations to ensure structural redundancy and balanced energy dissipation between compression and tension members: (a and c) poor configurations; (b and d) acceptable configurations

of their plane); these must then be designed to resist the maximum brace compression force in a stable manner while undergoing the large plastic rotations that result from brace buckling. Astaneh-Asl et al. (1986) suggested providing a clear distance of twice the plate thickness between the end of the brace and the assumed line of restraint for the gusset plate to permit plastic rotations and to preclude plate buckling (see Figure 9-15).

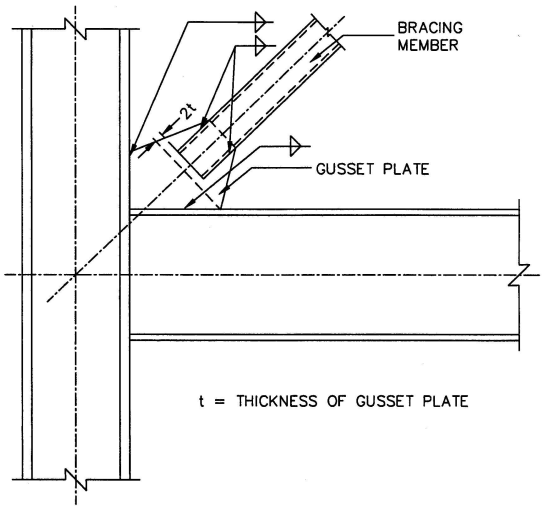

Figure 9-15. Brace-to-gusset connection detail to permit ductile out-of-plane brace buckling (AISC 1997, with permission from American Institute of Steel Construction, Chicago, Illinois)

9.3.5 Columns and Beams

Beams and columns in braced frames must be designed to remain elastic when all braces have reached their maximum tension or compression capacity ($1.1R_y$ times the nominal strength) to eliminate inelastic response in all components except for the braces. This requirement could be too severe for columns, however, as the braces along the height of a multistory frame do not necessarily reach their capacity simultaneously during an earthquake. Statistical approaches have been proposed to evaluate the maximum likely column load (Redwood and Channagiri 1991). The AISC Seismic Provisions address this issue using special load conditions described in Section 9.1, with the further specification that the maximum axial tension forces in columns need not be taken larger than the value corresponding to foundation uplift. For SCBFs, the Provisions also require that columns satisfy the same width-to-thickness ratio limits as braces (i.e., λ_{ps} in Table 9-2).

Partial penetration groove welds in column splices have been observed to fail in a brittle manner (Bruneau and Mahin 1990). When a welded column splice is expected to be in tension under the loading combination shown in Eq. 9-5, the AISC Seismic Provisions mandate that the partial joint penetration groove welded joints in SCBFs be designed to resist 200% of the strength required by elastic analysis using code-specified forces. Column splices also need to be designed to develop at least the nominal shear strength of the smaller connected member and 50% of the nominal flexural strength of the smaller connected section.

9.3.6 Special Bracing Configuration Requirements

Special requirements apply to the design of V-type and inverted V-type braced frames (also known as chevron braced frames). Because braces meet at the mid-span of beams in these frames, the vertical force resulting from the unequal compression and tension strengths of these braces can have a considerable impact on the cyclic behavior of the frame. That vertical force introduces flexure in the beam, and possibly a plastic hinge in the beam, producing the plastic collapse mechanism shown in Figure. 9-16. Therefore, it is imperative that beams in chevron braced frames be continuous between columns. It has also been observed that once a yielding mechanism develops in a chevron-type brace at a particular story, damage tends to concentrate at that story. A comprehensive discussion of the seismic behavior of chevron braced frames under seismic loading is beyond the scope of this chapter, and is presented elsewhere (Bruneau et al. 1997).

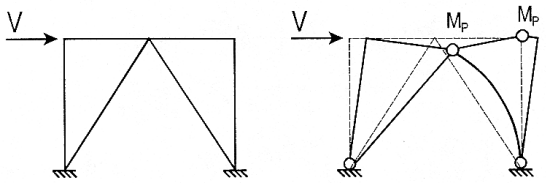

Figure 9-16. Plastic collapse mechanism of chevron braced frame having plastic hinge in beam

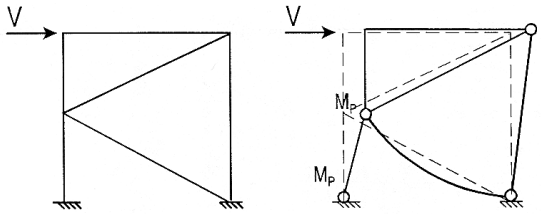

Figure 9-17. Plastic collapse mechanism of K-Braced frame with plastic hinge in column

Seismic provisions usually require that beams in chevron braced frames be capable of resisting their tributary gravity loads neglecting the presence of the braces. The AISC Seismic Provisions also require that each beam in an SCBF be designed to resist a maximum unbalanced vertical load calculated using full yield strength for the brace in tension, and 30% of the brace buckling strength in compression. In OCBFs, this latter provision need not be considered. However, braces in OCBFs must be designed to have 1.5 times the strength required by load combinations that include seismic forces, which is equivalent to designing chevron braced frames for a smaller value of R to compensate for their smaller ductility.

Finally, to prevent instability of a beam bottom flange at the intersection point of the braces in a chevron braced frame, in a manner similar to that shown in Figure 9-9b, the top and bottom flanges of beams in SCBFs and OCBFs must be designed to resist a lateral force equal to 2% of the nominal beam flange strength (i.e., $0.02A_fF_y$). This requirement is best met by the addition of a beam perpendicular to the chevron braced frame.

The above concepts also explain why a number of braced frame configurations are undesirable in seismic regions. For example, in a K-type braced frame (see Figure 9-17), the unequal buckling and tension-yielding strengths of the braces would create an unbalanced horizontal load at the mid-height of the columns, jeopardizing the ability of the column to carry gravity loads if a plastic hinge forms at the mid-height of the column.

9.4 Behavior and Design of Eccentrically Braced Frames

9.4.1 Introduction

While a properly designed and constructed steel moment frame can behave in a very ductile manner, moment frames are very flexible and their design is usually dictated by the drift limitations. Concentrically braced frames, on the other hand, have a large lateral stiffness, but their energy dissipation capacity is affected by brace buckling. In the early 1970s, an innovative steel system called the Eccentrically Braced Frame (EBF) that combines the advantages of both the steel moment frame and braced frame was proposed in Japan (Fujimoto et al. 1972, Tanabashi et al. 1974). The EBF dissipates energy by controlled yielding of shear or moment links. In the United Sates, the EBF system was first studied by Roeder and Popov (1978). This attractive system rapidly gained acceptance by the design profession (Teal 1979, Libby 1981, Merovich et al. 1982), some being constructed well before detailed design provisions were developed in the United States. In the 1980s, numerous studies on link behavior provided insight into the cyclic response of EBFs (Manheim and Popov 1983, Hjelmnstad and Popov 1983, 1984, Malley and Popov 1984, Kasai and Popov 1986a and 1986b, Ricles and Popov 1989, Engelhardt and Popov 1989). EBF design provisions were first promulgated in the 1988 Uniform Building Code. Experimental verifications of EBF response at the system level were also conducted in the mid- to late-1980s (Yang 1985, Roeder et al. 1987, Whittaker et al. 1989).

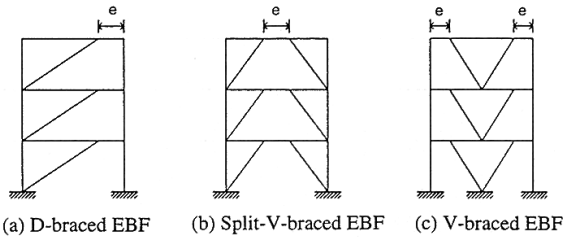

Figure 9-18. Typical EBF configurations

9.4.2 Basic Concept and EBF Behavior

An eccentrically braced frame is a framing system in which the axial force induced in the braces are transferred either to a column or another brace through shear and bending in a small segment of the beam. Typical EBF geometries are shown in Figure 9-18. The critical beam segment is called a "link" and is designated by its length, *e*. Links in EBFs act as structural fuses to dissipate the earthquake induced energy in a building in a stable manner. To serve its intended purpose, a link needs to be properly detailed to have adequate strength and stable energy dissipation. All the other structural components (beam segments outside of the link, braces, columns, and connections) are proportioned following capacity design provisions to remain essentially elastic during the design earthquake.

Elastic Stiffness

The variations of the lateral stiffness of a simple EBF with respect to the link length is shown in Figure 9-19 (Hjelmstad and Popov 1984). Note that *e/L* ratios of 0.0 and 1.0 correspond to a concentrically braced frame and a moment frame, respectively. The figure clearly shows the advantage of using a short link for drift control.

Link Deformation

Consider the idealized split V-type EBF in Figure 9-18b. Once the links have yielded in shear, the plastic mechanism shown in Figure 9-20a will form. Applying simple plastic theory, the kinematics of the plastic mechanism require that:

$$\gamma_p = \frac{L}{e}\theta_p \qquad (9\text{-}17)$$

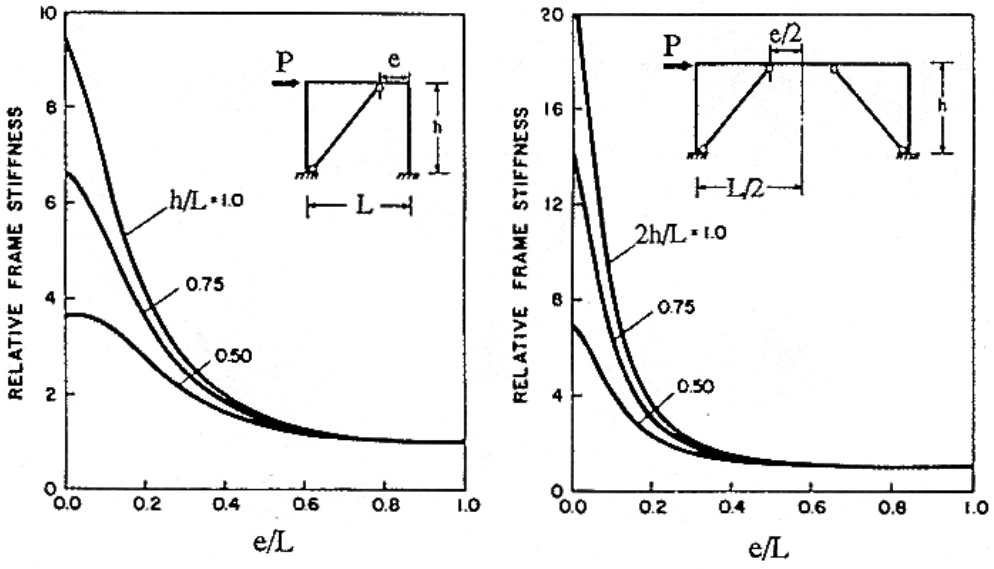

Figure 9-19. Variations of lateral stiffness with respect to link length (Hjelmstad and Popov 1994)

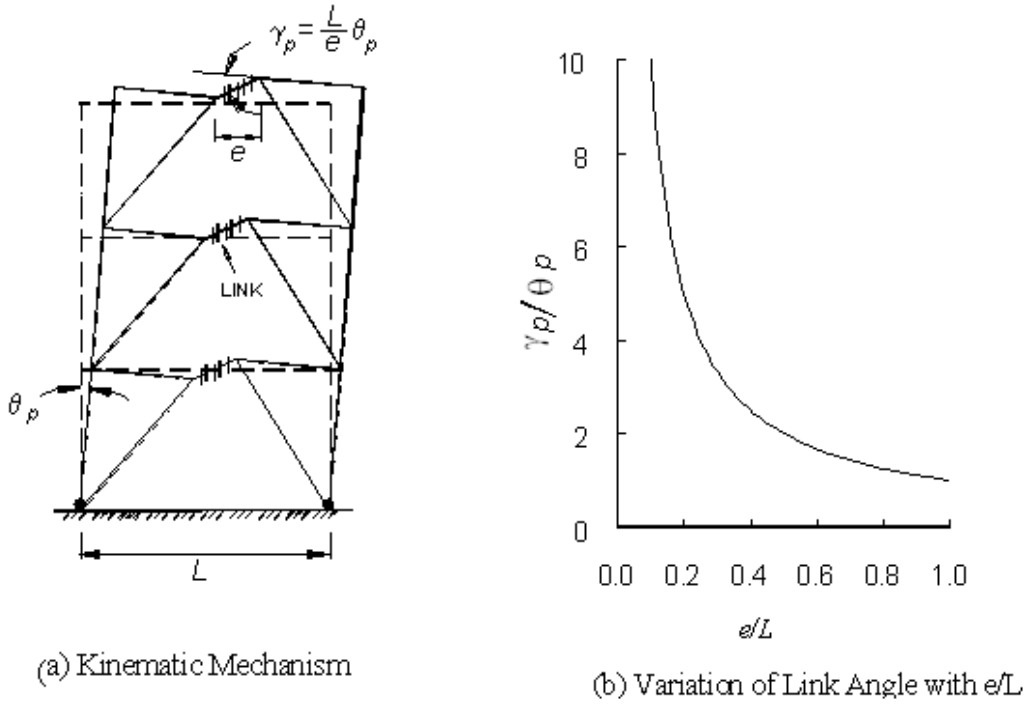

Figure 9-20. Kinematic mechanism and link plastic angle of a K-type EBF

where θ_p is the plastic drift angle (or plastic story drift ratio), and γ_p is the plastic deformation of the link. Based on Eq. 9-17, the variation of γ_p with respect to the link length is shown in Figure 9-20b. Because the elastic component of the total drift angle is generally small, the plastic story drift angle, θ_p, can be conservatively estimated as the total story drift divided by the story height, *h*:

$$\theta_p \approx \frac{\Delta_s}{h} = \frac{C_d \Delta_e}{h} \qquad (9\text{-}18)$$

where Δ_e is the story drift produced by the prescribed design earthquake force, and C_d (= 4) is the deflection amplification factor. To ensure that the deformation capacity of the link is not exceeded, it is obvious from Eq. 9-17 that the link length cannot be too short. Note that the kink that forms between the link and the beam outside the link also implies damage of the concrete slab at the ends of the link.

Ultimate Strength

Unless architectural considerations dictate otherwise, a short link is usually used so that the link will yield primarily in shear. The lateral strength of such an EBF can then be calculated conveniently using simple plastic theory. Assuming that the link behaves in an elastic-perfectly plastic manner, the lateral strength, P_u, of the simple one-story split V-shaped EBF frame can be computed by equating the external work to the internal work:

$$\text{External work} = P_u (h\theta_p) \qquad (9\text{-}19a)$$

$$\text{Internal work} = \int_0^e V_p \gamma_p dx = e V_p \gamma_p \qquad (9\text{-}19b)$$

where V_p is the shear strength of the link. Substituting Eq. 9-17 into Eq. 9-19b, the resulting ultimate strength of the EBF frame is

$$P_u = \frac{V_p L}{h} \qquad (9\text{-}20)$$

As long as the link yields in shear, the above equation shows that the ultimate strength is independent of the link length. This simple plastic theory can also be applied to multistory frames (Kasai and Popov 1985).

Once the link length exceeds a threshold value, flexure and shear dominates the link strength. The ultimate strength of the frame then decreases with an increase in link length. Figure 9-21 illustrates the strength variations. This figure also indicates that the ultimate strength of an EBF with short links is significantly larger than that of a moment frame (i.e., $e/L = 1.0$).

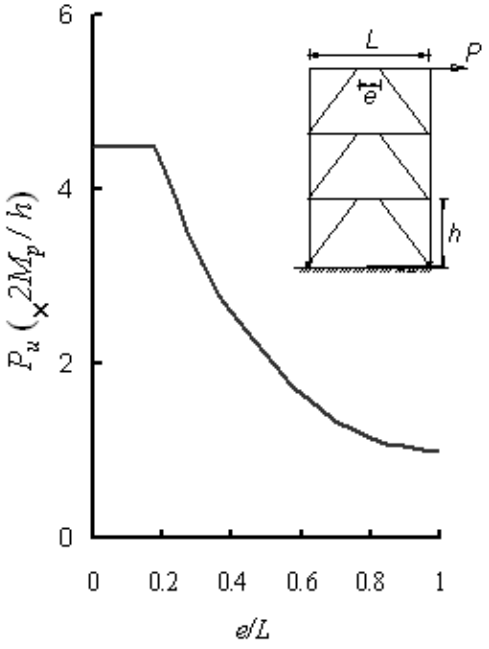

Figure 9-21. Variations of EBF ultimate strength with *e/L* (Kasai and Popov 1985)

9.4.3 Link Behavior

Critical Length for Shear Link

Figure 9-22 shows the free-body diagram of a link. Ignoring the effects of axial force and the interaction between moment and shear in the link, flexural hinges form at two ends of the link when both M_A and M_B reach the plastic moment, M_p. A shear hinge is said to form when the shear reaches V_p. The plastic moment and shear capacities are respectively computed as follows:

$$M_p = F_y Z \tag{9-21a}$$

$$V_p = 0.6F_y(d - 2t_f)t_w \tag{9-21b}$$

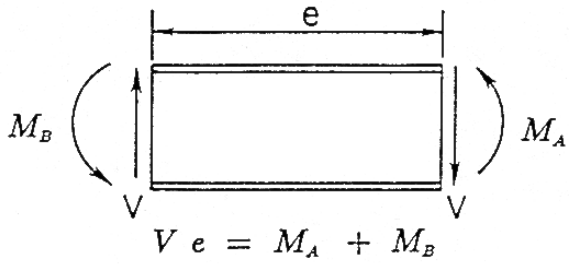

Figure 9-22. Link deformation and free-body diagram

A balanced yielding condition corresponds to the simultaneous formation of flexural hinges and a shear hinge. The corresponding link length is

$$e_0 = \frac{2M_p}{V_p} \tag{9-22}$$

In a short link ($e \le e_0$), a shear hinge will form. When $e > e_0$, a flexural (or moment) hinge forms at both ends of the link, and the corresponding shear force is:

$$V = \frac{2M_p}{e} \tag{9-23}$$

Based on plastic theory, Eq. 9-22 can be modified slightly to include the effect of interaction between M and V. Nevertheless, experimental results indicated that the interaction is weak and that such interaction can be ignored (Kasai and Popov 196b). Test results also showed that a properly stiffened short link can strain harden and develop a shear strength equal to $1.5V_p$. The end moments of a link that has yielded in shear can continue to increase

due to strain hardening and, therefore, flexural hinges can develop. To avoid low-cycle fatigue failure of the link flanges due to high strains, these end moments are limited to $1.2M_p$, and the maximum length (e_0 in Eq. 9-22) for a shear link was modified as follows (Kasai and Popov 1986b):

$$e_0 = \frac{2(1.2M_p)}{1.5V_p} = \frac{1.6M_p}{V_p} \qquad (9\text{-}24)$$

Longer Links

Experimental results have shown that the inelastic deformation capacity of an EBF can be greatly reduced when long links ($e > e_0$) are used. Following the above logic, it can be shown that flexural hinges dominate the link response when e is larger than $2.6M_p/V_p$. In the transition region where $1.6M_p/V_p < e < 2.6M_p/V_p$, the link undergoes simultaneous shear and flexural yielding (Engelhardt and Popov 1989). Figure 9-23 classifies links in EBFs. Note that when longer links are used in the D-type or V-type EBF (see Figure 9-18), the welded connection between the link and the column is subjected to high moments and it could be vulnerable to brittle fracture if detailed similar to the connections that failed during the Northridge earthquake (see Section 9.2).

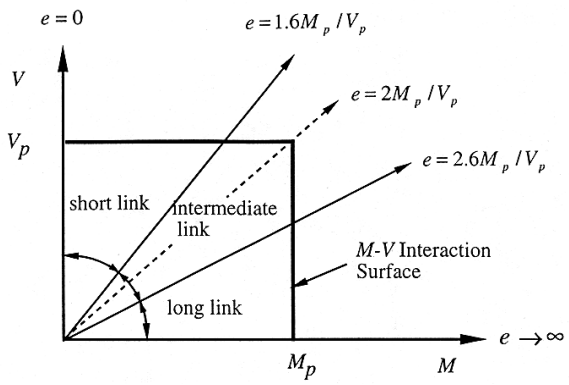

Figure 9-23. Classification of links

Based on experimental results, the link deformation capacity, γ_a, as given by the AISC Seismic Provisions is shown in Figure 9-24. The calculated rotation angle, γ_p, cannot exceed γ_a.

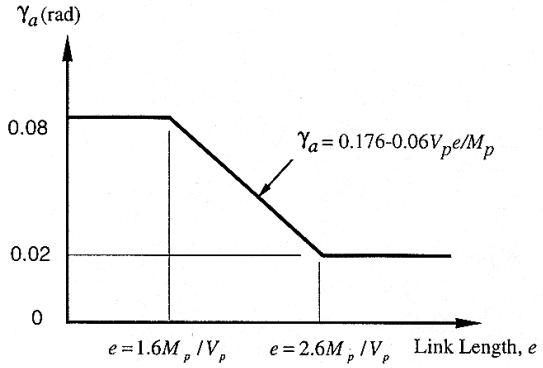

Figure 9-24. Allowable link angles per AISC Seismic Provisions (1997)

Effect of Axial Force

The presence of an axial force in a link reduces not only the flexural and shear capacities but also its inelastic deformation capacity (Kasai and Popov 1986b). When the axial force, P_u, exceeds 15% of the yield force, $P_y (= A_g F_y)$, the P-M interaction formula for plastic design (AISC 1989) can be used to compute the reduced plastic moment, M_{pa}:

$$M_{pa} = 1.18M_p\left(1 - \frac{P_u}{P_y}\right) \qquad (9\text{-}25)$$

The reduced shear capacity is (Manheim and Popov 1983):

$$V_{pa} = V_p\sqrt{1-(P_u/P_y)^2} \qquad (9\text{-}26)$$

Replacing M_p and V_p in Eq. 9-24 by M_{pa} and V_{pa}, the reduced value of e_0 when $\rho A_w/A_g \geq 0.3$ can be approximated as follows (Kasai and Popov 1986b):

$$e_0 = \left(1.15 - 0.5\rho' \frac{A_w}{A_g}\right) \frac{1.6M_p}{V_p} \qquad (9\text{-}27)$$

where $\rho' = P/V$, and $A_w = (d - 2t_f)t_w$. The correction is unnecessary if $\rho' A_w / A_g < 0.3$, in which case the AISC Seismic Provisions (1997) require that the link length shall not exceed that given by Eq. 9-24.

Effect of Concrete Slab

Research conducted on composite links showed that composite action can significantly increase the link shear capacity during the first cycles of large inelastic deformations. However, composite action deteriorates rapidly in subsequent cycles due to local concrete floor damage at both ends of the link (Ricles and Popov 1989). For design purposes, it is conservative to ignore the contribution of composite action for calculating the link shear strength. But the overstrength produced by the composite slab effect needs to be considered when estimating the maximum forces that the shear link imposes to other structural components (Whittaker et al. 1989).

Link Detailing

Full-depth web stiffeners must be placed symmetrically on both sides of the link web at the diagonal brace ends of the link. These end stiffeners are required to have a combined width not less than ($b_f - 2t_w$) and a thickness not less than $0.75t_w$ nor 3/8 inch, whichever is larger.

The link section needs to satisfy the same compactness requirement as the beam section for special moment frames. Further, the link needs to be stiffened in order to delay the onset of web buckling and to prevent flange local buckling. The stiffening requirement is dependent on the length of link (see Figure 9-23). For a shear link with $e \le 1.6M_p/V_p$, a relationship among the link web deformation angle, the web panel aspect ratio as well as the beam web slenderness ratio was developed (Kasai and Popov 1986a). A conservative approximation of the relationship follows:

$$a = C_B t_w - \frac{d}{5} \qquad (9\text{-}28)$$

where a = stiffener spacing, d = link depth, t_w = link web thickness, and C_B = 56, 38, and 29 for γ_p = 0.03, 0.06, and 0.09 radian, respectively. These C_B values are slightly modified and are adopted in the AISC Seismic Provisions (1997) as follows:

(1) When $e \le 1.6M_p/V_p$, intermediate stiffeners are needed per Eq. 9-28, but the coefficient C_B is a function of the deformation demand; the relationship between C_B and γ_p implied by the AISC Seismic Provisions is shown in Figure 9-25.

(2) When $2.6M_p/V_p \le e \le 5M_p/V_p$, intermediate stiffeners shall be provided at a distance $1.5b_f$ from each end of the link to control flange local buckling.

(3) When $1.6M_p/V_p \le e \le 2.6M_p/V_p$, intermediate stiffeners satisfying the requirements of both Cases 1 and 2 are needed.

(4) When $e > 5M_p/V_p$, intermediate stiffeners are not required.

Intermediate link web stiffeners must be full depth. While two-sided stiffeners are required at the end of the link where the diagonal brace intersects the link, intermediate stiffeners placed on one side of the link web are sufficient for links less than 25 inches in depth. Fillet welds connecting a link stiffener

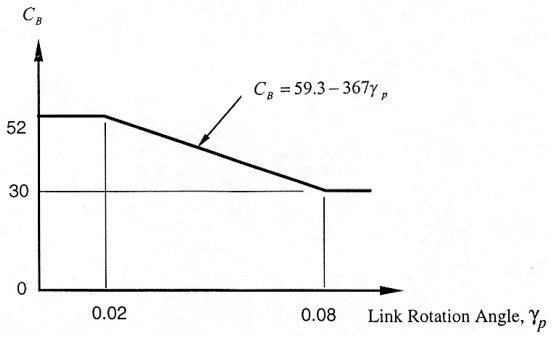

Figure 9-25. Variation of C_B

to the link web shall have a design strength to resist a force of $A_{st}F_y$, where A_{st} is the stiffener area. The design strength of fillet welds fastening the stiffener to the flanges shall be adequate to resist a force of $A_{st}F_y/4$.

Lateral Bracing of Link

To ensure stable hysteresis, a link must be laterally braced at each end to avoid out-of-plane twisting. Lateral bracing also stabilizes the eccentric bracing and the beam segment outside the link. The concrete slab alone cannot be relied upon to provide lateral bracing. Therefore, both top and bottom flanges of the link beam must be braced. The bracing should be designed for 6 percent of the expected link flange strength, $R_yF_yb_ft_f$.

9.4.4 Capacity Design of Other Structural Components

Links in an EBF are designated as structural fuses and are sized for code-specified design seismic forces. All other elements (beam segments outside the link, braces, columns, and connections) are then designed for the forces generated by the actual (or expected) capacity of the links rather than the code-specified design seismic forces. The capacity design concept thus requires that the computation of the link strength not only be based on the expected yield strength of the steel but also includes the consideration of strain-hardening and overstrength due to composite action of the slab.

Diagonal Brace

The required axial and flexural strength of the diagonal brace shall be those generated by the expected shear strength of the link R_yV_n increased by 125 percent to account for strain-hardening. The nominal shear capacity, V_n, is the lesser of V_p or $2M_p/e$. Although braces are not expected to experience buckling, the AISC Seismic Provisions take a conservative approach by requiring that a compact section ($\lambda < \lambda_p$) be used for the brace.

At the connection between the diagonal brace and the beam, the intersection of the brace and beam centerlines shall be at the end of the link or within the length of the link (see Figure 9-26a). If the intersection point lies outside the link length, the eccentricity together with the brace axial force produces additional moments in the beam and brace.

The diagonal brace-to-beam connection at the link end of the brace shall also be designed to develop the expected strength of the brace. No part of this connection shall extend over the link length to reduce the link length, e. If the connection is designed as a pin (see Figure. 9-26b), the gusset plate needs to be properly stiffened at the free edge to avoid local buckling (Roeder et al. 1989).

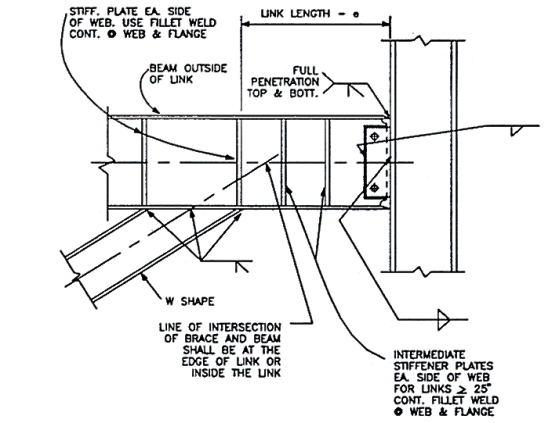

(a) Diagonal Brace Fully Connected to Link

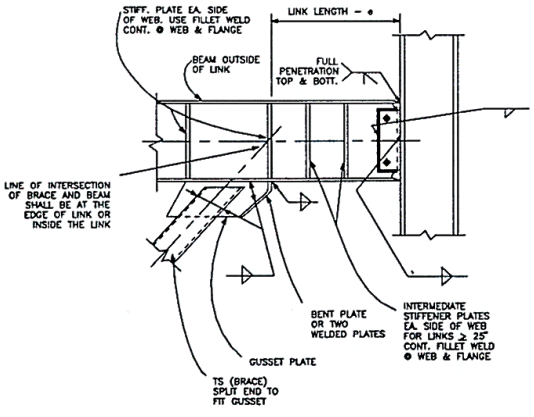

(b) Diagonal Brace Pin-Connected to Link

Figure 9-26. EBF link and connection details (AISC 1997)

Link-to-Column Connections

Of the common EBF configurations shown in Figure 9-18, it is highly desirable to use the split V-braced EBF in order to avoid the moment connection between the link and column. Prior to the 1994 Northridge earthquake, test results showed that the fully restrained welded connection between the column and the link (especially longer links) is vulnerable to brittle fracture similar to those found in the beam-to-column moment connections after the Northridge earthquake. Therefore, the AISC Seismic Provisions (1997) require that the deformation capacity of the link-to-column connections be verified by qualifying cyclic tests. Test results shall demonstrate that the link inelastic rotation capacity is at least 20 percent greater than that calculated by Eq. 9-17.

When reinforcements like cover plates are used to reinforce the link-to-column connection, the link over the reinforced length may not yield. Under such circumstances, the link is defined as the segment between the end of the reinforcement and the brace connection. Cyclic testing is not needed when (1) the shortened link length does not exceed e_o in Eq. 9-24, and (2) the design strength of the reinforced connection is equal to or greater than the force produced by a shear force of 1.25 $R_y V_n$ in the link.

Tests also demonstrated that the welded connections of links to the weak-axis of a column were vulnerable to brittle fracture (Engelhardt and Popov 1989); this type of connection should be avoided.

Beam-to-Column Connection

For the preferred EBF configuration where the link is not adjacent to a column, a simple framing connection between the beam and the column is considered adequate if it provides some restraint against torsion in the beam. The AISC Seismic Provisions stipulate that the magnitude of this torsion be calculated by considering perpendicular forces equal to 2 percent of the beam flange nominal strength, $F_y b_f t_f$, applied in opposite directions on each flange.

Beam Outside of Link

The link end moment is distributed between the brace and the beam outside of the link according to their relative stiffness. In preliminary design, it is conservative to assume that all the link end moment is resisted by the beam. The link end moment shall be calculated using 1.1 times the expected nominal shear strength ($R_y V_n$) of the link. Because a continuous member is generally used for both the link and the beam outside the link, it is too conservative to use the expected yield strength ($R_y F_y$) for estimating the force demand produced by the link while the beam strength is based on the nominal yield strength (F_y). Therefore, the AISC Seismic Provisions allow designers to increase the design strength of the beam by a factor R_y.

The horizontal component of the brace produces a significant axial force in the beam, particularly if the angle between the diagonal brace and the beam is small. Therefore, the beam outside the link needs to be designed as a beam-column. When lateral bracing is used to increase the capacity of the beam-column, this bracing must be designed to resist 2 percent of the beam flange nominal strength, $F_y b_f t_f$.

Column

Using a capacity design approach, columns in braced bays shall have a sufficient strength to resist the sum of gravity-load actions and the moments and axial forces generated by 1.1 times the expected nominal strength ($R_y V_n$) of the link. This procedure assumes that all links will yield and reach their maximum strengths simultaneously. Nevertheless, available multistory EBF test results showed that this preferred yielding mechanism is difficult to develop. For example, shaking table testing of a 6-story reduced scale EBF model showed that

links in the bottom two stories dissipated most of the energy (Whittaker et al. 1989). Therefore, this design procedure may be appropriate for low-rise buildings and the upper stories of medium- and high-rise buildings but may be too conservative in other instances.

The alternative design procedure permitted by the AISC Seismic Provisions is to amplify the design seismic axial forces and moments in columns by the overstrength factor, Ω_o (= 2.0, see Table 9-1). See Eqs. 9-4 and 9-5 for the load combinations. The computed column forces need not exceed those computed by the first procedure. Therefore, the first design procedure will generally produce a more conservative design for columns.

9.5 Design Examples

9.5.1 General

A six-story office building having the floor plan shown in Figure 9-27 is used to

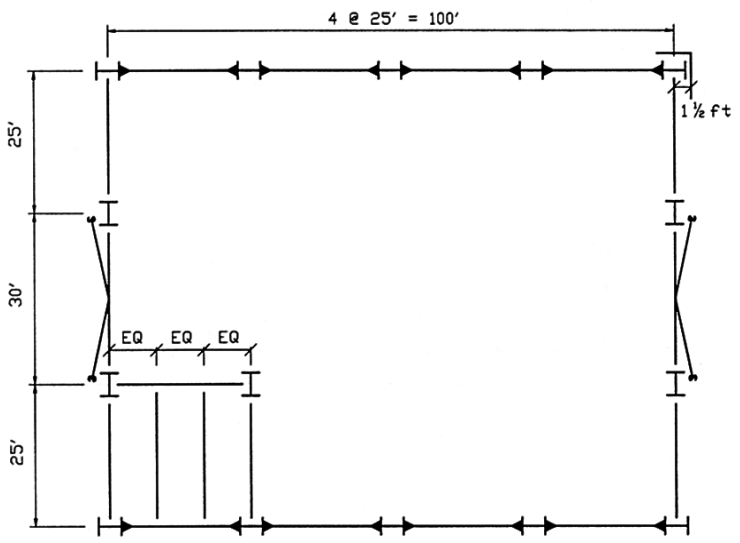

(a) Floor Framing Plan

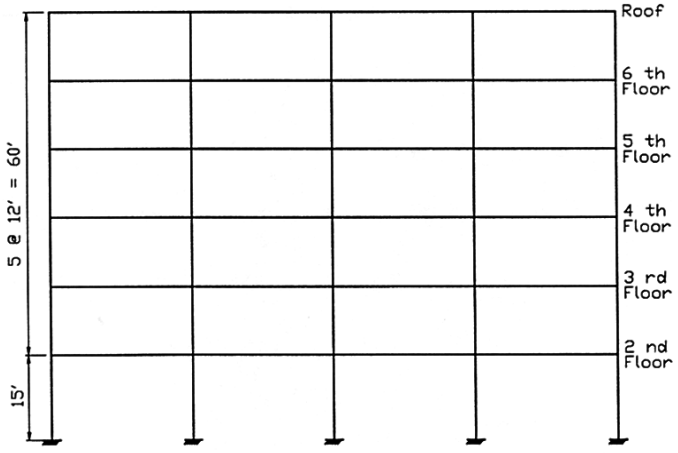

(b) Moment Frame Elevation

Figure 9-27. A six-story office building

demonstrate the seismic design procedures. The design follows the AISC Seismic Provisions (1997) and the Load and Resistance Factor Design Specification for Structural Steel Buildings (1993). Special Moment-Resisting Frames (SMFs) are used in the E-W direction, and their design is presented in Section 9.5.2. Braced frames provide lateral load-resistance in the N-S direction; these are designed as Special Concentrically Braced Frames (SCBFs) in Section 9.5.3 and Eccentrically Braced Frames (EBFs) in Section 9.5.4, respectively.

The design gravity loads are listed in Table 9-3. The NEHRP Recommended Provisions (1997) are the basis for computing the design seismic forces. It is assumed that the building is located in a high seismic region with the following design parameters:

S_S = 1.5 g
S_1 = 0.6 g
Site Class = B
I = 1.0 (Seismic User Group I)
Seismic Design Category = D

The design response spectrum is shown in Figure 9-28.

The design follows the Equivalent Lateral Force Procedure of the NEHRP Recommended Provisions. The design base shear ratio, C_s, is computed as follows:

$$C_s = \frac{S_{D1}}{T(R/I)} \le \frac{S_{DS}}{(R/I)} \qquad (9\text{-}29)$$

where S_{D1} (= 0.4 g) and S_{DS} (= 1.0 g) are the design spectral response accelerations at a period of 1.0 second and in the short period range, respectively. The values of R for the three framing systems considered in this example are listed in Table 9-4. The NEHRP empirical period formula is used to compute the approximate fundamental period, T_a:

$$T_a = C_T h_n^{3/4} \qquad (9\text{-}30)$$

where h_n (ft) is the building height, and the coefficient C_T is equal to 0.035, 0.030, and 0.02 for SMFs, EBFs, and SCBFs, respectively. Alternatively, the value of T obtained from a dynamic analysis can be used in design, but the period thus obtained cannot be taken larger than $C_u T_a$ for the calculation of required structural strengths, where C_u = 1.2

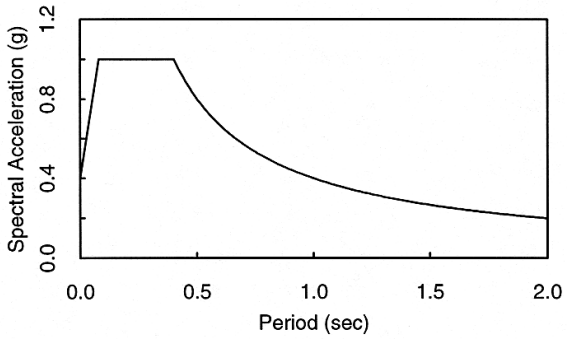

Figure 9-28. Elastic design response spectrum

for this design example. To establish seismic forces for story drift computations, however, this upper limit is waived by the NEHRP Recommended Provisions. Recognizing that the analytically predicted period of a multistory SMF is generally larger than $C_u T_a$, this upper bound value is used to compute the design base shear ratio for preliminary design. Based on Eq. 9-1, the design base shear ratios for the three types of frames are listed in Table 9-4.

The following two load combinations are to be considered:

$$1.2D + 0.5L + 1.0E \qquad (9\text{-}31)$$

$$0.9D - 1.0E \qquad (9\text{-}32)$$

where $E = \rho Q_E + 0.2\, S_{DS} D$. The Redundancy Factor, ρ, is

$$\rho = 2 - \frac{20}{r_{\max}\sqrt{A}} = 2 - \frac{20}{0.25\sqrt{8549}} = 1.13 \qquad (9\text{-}33)$$

(See the NEHRP Recommended Provisions on ρ.) Therefore, the above two load combinations can be expressed as

Table 9-3. Design gravity loads

Load	Dead Load (psf)	Live Load [+](psf)
Roof	70	20
Floor	90[*]	50
Cladding	20	-

*80 psf for computing reactive weight.
+ Use $L = L_0\left(0.25 + 15/\sqrt{A_I}\right)$ for live load reduction (ASCE 1998)

Table 9-4. System parameters and design base shears

Framing System	R	Ω_o	C_d	T_a (sec)	C_s	V_B* (kip)	k
SMF	8	3	5 ½	1.07	0.047	111	1.285
SCBF	6	2	5	0.51	0.131	305	1.0
EBF	8	2	4	0.76	0.066	156	1.13

*Values have been increased by 5% to account for accidental eccentricity.

$$1.2D + 0.5L + 1.0(\rho Q_E + 0.2D)$$

$$= 1.4D + 0.5L + \rho Q_E \qquad (9\text{-}34)$$

$$0.9D - 1.0(\rho Q_E + 0.2D) = 0.7D - \rho Q_E \qquad (9\text{-}35)$$

The design base shear, V_B (= $C_s W$, where W = building reactive weight), for computing the seismic effect (Q_E) is distributed to each floor level as follows:

$$F_x = \frac{W_x h_x^k}{\sum W_i h_i^k} V_B \qquad (9\text{-}36)$$

where the values of k listed in Table 9-4 are used to consider the higher-mode effect. Based on Eq. 9-36, the design story shears for each example frame are summarized in Table 9-5.

9.5.2 Special Moment Frames (SMF)

Story Shear Distribution

The story shear distribution of the SMF listed in Table 9-5 is for strength computations. To compute story drift, however, it is permissible to use the actual fundamental period, T, of the structure. The actual period of this 6-story SMF is expected to be larger than the approximate period, T_a (= 1.07 seconds), determined from Eq. 9-30. There exists many approaches to the preliminary design of SMF. The one followed in this section has been proposed by Becker (1997). First, the fundamental period can be estimated using a simplified Rayleigh method (Teal 1975):

$$T = 0.25\sqrt{\frac{\Delta_r}{C_1}} \qquad (9\text{-}37)$$

where
T = fundamental period,
Δ_r = lateral deflection at the top of the building under the lateral load V,
$C_1 = V/W$,
V = lateral force producing deflection, and
W = building reactive weight.

The story drift requirement is:

$$\delta_x = \frac{C_d \Delta}{I} < 0.02H,$$

$$\Delta_r < \frac{0.02HI}{C_d} = \frac{0.02 \times 75 \times 12}{5.5} = 3.27 \text{ in}$$

Assuming conservatively that the total deflection is about 60% of the allowable value,

$$\Delta_r = 0.60(3.27) = 1.96 \text{ in}$$

Table 9-5. Design story shears

Floor	W_i (kips)	h_i (ft)	Story Shear* (kips)		
			SMF	SCBF	EBF
R	322	75	34	84	45
6	387	63	67	168	90
5	387	51	92	236	125
4	387	39	109	288	150
3	387	27	120	324	167
2	392	15	125	345	176

*ρ (= 1.13) is included.

$$C_1 = 1.05\rho(C_s) = 1.05(1.13)\frac{0.4}{T(R/I)} = \frac{0.059}{T}$$

(where 1.05 accounts for torsion)

$$T = 0.25\sqrt{\frac{1.96}{0.059/T}} = 1.44\sqrt{T}$$

Solving the above equation gives a value of T equal to 2.0 seconds. For this value, however,

$$C_s = \frac{S_{D1}}{T(R/I)} = \frac{0.4}{2(8/1.0)},$$
$$= 0.025 < 0.044\,S_{DS}$$

and $C_s = 0.044$ controls. That is, the minimum seismic base shear for drift computations is

$$V = 1.05 \times \rho \times 0.044W = 0.052W$$

Since the base shear ratios for strength and drift designs are 0.047 and 0.044, respectively, a scaling factor of 0.94 (= 0.044/0.047) can be used to reduce the story shears listed in Table 9-5 for drift computations.

Member Proportions

For brevity in this design example, detailed calculations are presented only for the beams on the fourth floor and the columns above and below that floor (see Figure 9-29). The portal method is used for preliminary design. Assuming that the point of inflection occurs at the mid-length of each member:

$$2F_1 + 3F_2 = 0.94(109) = 102.5 \text{ kips}$$

$$F_1 = F_2/2, \quad F_2 = 25.6 \text{ kips}$$

Consider the interior beam-column assembly shown in Figure 9-29. Summing the moments at the point of inflection at point P, the beam shear, F_3, is calculated to be:

$$12F_2 = 25F_3, \quad F_3 = 12.3 \text{ kips}$$

The story drift due to column and girder deformations is:

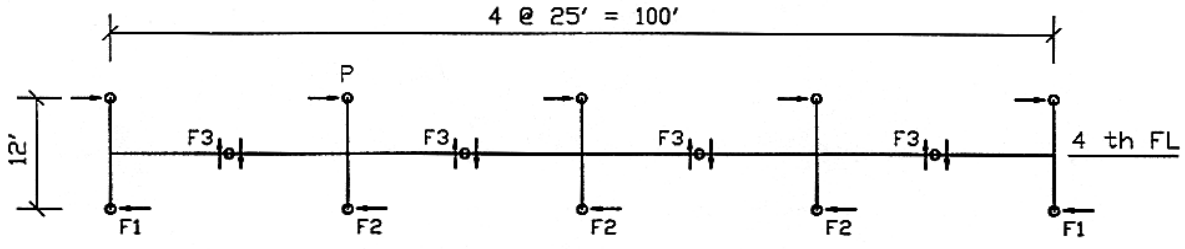

Figure 9-29. Typical shear force distributions in beams and columns

$$\Delta = \Delta_c + \Delta_g = \frac{F_2 h^3}{12EI_c} + \frac{F_2 L h^2}{12EI_g} \qquad (9\text{-}38)$$

where
Δ = story drift,
Δ_c = drift produced by column deformation,
Δ_g = drift produced by beam deformations,
F_2 = column shear,
h = story height,
L = beam length between points of inflection,
I_c = moment of inertia of column, and
I_g = moment of inertia of beam.

Eq. 9-38 uses centerline dimensions and ignores the shear and axial deformations of the beams and column. In equating Eq. 9-38 to the allowable drift, it is assumed that the panel zone deformation will contribute 15% to the story drift; the actual contribution of the panel zone deformation will be verified later.

$$\delta_x = \frac{C_d \Delta}{I} \le (0.85)0.02h,$$
$$\Delta \le 0.0031h = 0.45\,\text{in}$$

$$\frac{F_2 h^2}{12E}\left(\frac{h}{I_c} + \frac{L}{I_g}\right) \le 0.45 \qquad (9\text{-}39)$$

The above relationship dictates the stiffness required for both the beams and columns in order to meet the story drift requirement. By setting $I = I_c = I$ as a first attempt, Eq. 9-39 gives a required I = 1532 in^4. Using A992 steel for both the columns and the beams, it is possible to select W14×132 columns (I_c = 1530 in^4) and W24×62 beams (I_g = 1532 in^4).

In addition to satisfying the story drift requirements, the strength of the columns and beams also need to be checked for the forces produced by the normal seismic load combinations (Eqs. 9-34 and 9-35). However, beam and column sizes of this 6-story SMF are generally governed by the story drift and strong-column weak-girder requirements. Therefore, the strength evaluations of these members are not presented here.

A formal check of the strong column-weak beam requirement will be performed later. A quick check of this requirement for the flexural strength of both the beams and columns is worthwhile before the moment connections are designed. It is assumed that the column axial stress (P_u / A_g) is equal to $0.15F_y$. Beams are designed using the reduced beam section strategy in this example. Assuming that (1) the reduced beam plastic sectional modulus (Z_{RBS}) is 70% of the beam plastic sectional modulus (Z_{BM}), and (2) the moment gradient (M_v) from the plastic hinge location to the column centerline is 15% of the design plastic moment at the plastic hinge location:

$$\sum M^*_{pc} = 2[Z_c(F_y - P_u/A_g)] \approx 2\,(0.85 Z_C F_y)$$

$$Z_{RBS} \approx 0.7 Z_{BM}\,,\; M_v \approx 0.15(1.1 R_y Z_{RBS} F_y)$$

$$\begin{aligned}\sum M^*_{pb} &= 2[1.1 R_y\, Z_{RBS} F_y + M_v] \\ &\approx 2\left(1.1 R_y\, Z_{RBS} F_y \times 1.15\right) \\ &\approx 2(1.1\times 1.1\times 0.7\times 1.15 Z_{BM} F_y) \\ &= 2(0.97) Z_{BM} F_y\end{aligned}$$

To satisfy Eq. 9-14:

$$\frac{\sum M^*_{pc}}{\sum M^*_b} = \frac{2(0.85 Z_C)}{2(0.97 Z_{BM})} \ge 1.0$$

$$\frac{Z_C}{Z_{BM}} \ge 1.15$$

For the beam and column sizes selected:

$$\frac{Z_C}{Z_{BM}} = \frac{234}{153} = 1.53 \ge 1.15 \qquad \text{(OK)}$$

Both W14×132 and W24×62 satisfy the λ_{ps} requirements given in Table 9-2. Since the RBS is to be used, additional check of the beam web compactness is required:

$$\frac{h}{t_w} = 50.1 < \frac{418}{\sqrt{F_y}} = 59.1 \qquad \text{(OK)}$$

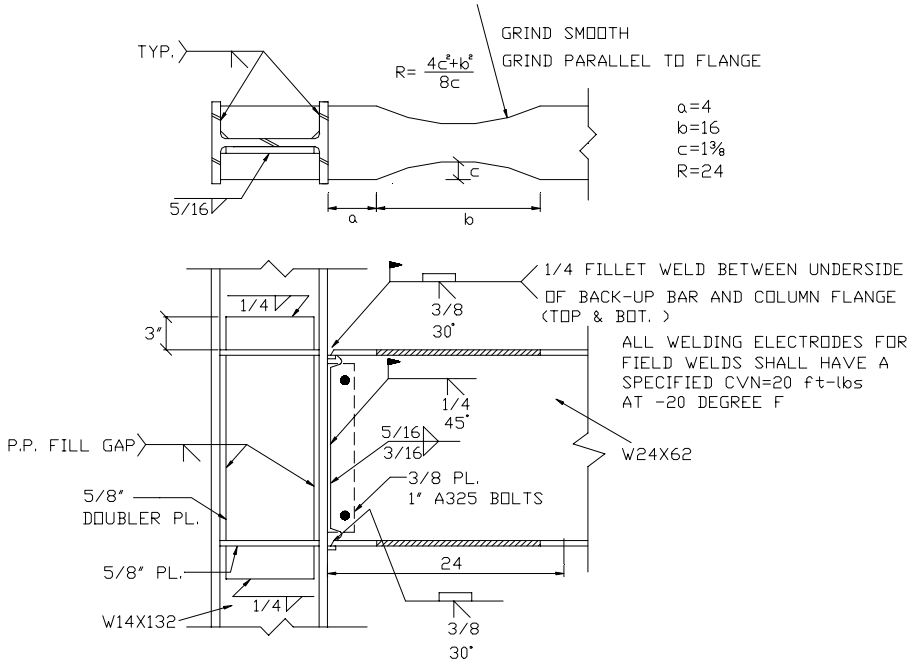

Figure 9-30. Reduced beam section and the welded beam-column connection details.

Beam-to-Column Connection Design

Reduced beam section details employing radius-cut (Figure 9-30) is the most promising beam-to-column connection detail. The key dimensions of the radius cut include the distance from the face of the column (dimension *a*), the length of the cut (dimension *b*), and the depth of the cut (dimension *c*). To minimize the moment gradient between the narrowest section and the face of column, the dimensions *a* and *b* should be kept small. However, making these dimensions too short may result in high strains either at the face of column or within the reduced beam sections. It has been recommended that (Engelhardt et al. 1996):

$a \approx (0.5 \text{ to } 0.75)b_f$
$b \approx (0.65 \text{ to } 0.85)d$

$$c \geq \frac{Z}{2t_f(d-t_f)}\left[1-\frac{\alpha(L-a-0.5b)}{1.1L}\right] \leq 0.25b_f$$

where L (= 142.7 in) is the distance from the face of the column to the point of inflection in the beam, b_f, t_f and d are flange width, flange thickness and beam depth, respectively. To determine the maximum cut dimension, c, it is assumed that the strain-hardened plastic moment developed at the narrowest beam section is equal to 1.1 times the plastic moment of the reduced section ($Z_{RBS}F_{ye}$). The factor 1.1 accounts for strain hardening. The factor α limits the beam moment (αM_p) developed at the face of column. The maximum value of α should range between 0.85 and 1.0. Based on an α equal to 0.90,

$a = 4.0 \text{ in} = 0.57b_f$
$b = 16 \text{ in} = 0.67d$
$c = 1.375 \text{ in} \approx 0.20b_f$

$$R = \frac{4c^2 + b^2}{8c} = 24 \text{ in}$$

Following the SAC Interim Guidelines (SAC 1997), other features of the connection include the use of notch-toughness weld metal, the use of a welded web connection, and the use of continuity plates. Lateral supports capable of resisting a minimum of 2% of the unreduced flange force should be provided such that the unbraced length is no larger than the following (see Figure 9-31):

$$L_b = \frac{2500}{F_y} r_y = \frac{2500}{50}(1.38) = 69 \text{ in} = 5.75 \text{ ft}$$

Additional bracing near the RBS is unnecessary because deep section is not used for the column.

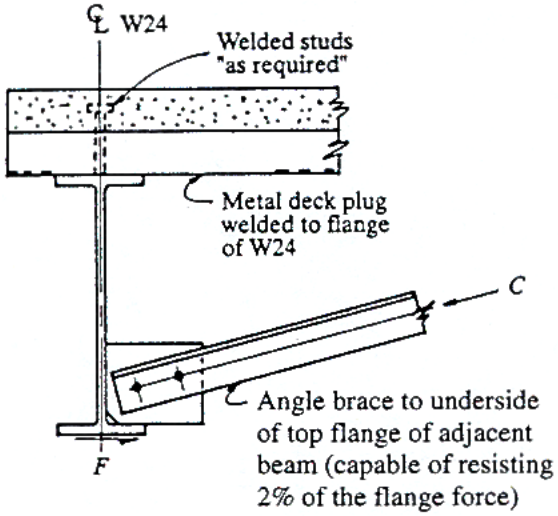

Figure 9-31. Lateral support for the beam

Strong Column-Weak Beam Criterion

The axial force in interior columns in a moment frame, produced by seismic loading, can be ignored generally. The axial force due to dead load on the upper floors, roof, and cladding is:

P_D = roof + (4 to 6)floors + cladding

= (25×14)(0.07)+3(25×14)(0.09)

+(25×12)(0.02) = 125 kips

and the live load axial force, including live load reduction, is

$$L = L_D\left(0.25 + \frac{15}{\sqrt{4(4)(25\times14)}}\right) = 22.5 \text{ psf}$$

P_L= 3(25×14)(0.0225)+(25×14)(0.02×0.45)

= 26.8 kips

Therefore, the factored axial load is

P_u = 1.4(125)+0.5(26.8) = 188 kips

The column moment capacity is

$$\sum M^*_{pc} = \sum Z_c (F_{yc} - P_{uc}/A_g)$$

= 2(234)(50-188/38.8)

= 21132 kip-in

The plastic sectional modulus of the RBS is

$$Z_{RBS} = Z_{BM} - 2ct_f(d - t_f)$$

$$= 153 - 2(1.375)(23.74 - 0.59) = 115 \text{ in}^4$$

The design plastic moment capacity of the reduced beam section is

$$M_{pd} = 1.1R_y Z_{RBS} F_y$$

$$= 1.1\times1.1\times115\times50 = 6958 \text{ kip} - \text{in}$$

and the corresponding beam shear is

$$V_{pd} = \frac{1.1R_y Z_{RBS} F_y}{[0.5(25\times12) - d_c/2 - a - b/2]}$$

= 53 kips

After extrapolating the beam moment at the plastic hinge location to the column center-line, the beam moment demand is

$$\sum M^*_{pb} = \sum (M_{pd} + M_v)$$

$$= \sum [M_{pd} + V_{pd}(d_c/2 + a + b/2)]$$

$$= 2\left[26958 + 53\left(\frac{14.66}{2} + 4 + 8\right)\right]$$

= 15965 kip-in

$$\frac{\sum M^*_{pc}}{\sum M^*_{pb}} = 1.32 > 1.0 \qquad \text{(OK)}$$

Therefore, the strong column-weak beam condition is satisfied.

Panel Zone Design

The unbalanced beam moment, ΔM, for the panel zone design is determined from the special load combination in Eq. 9-4, where the beam moment at the column face produced by $\Omega_o(\rho Q_E)$ is

$$M_1 = M_2 = \Omega_o (F_3/0.94)L$$

$$= 3.0(12.3/0.94)142.7 = 5602 \text{ kip-in}$$

$$\Delta M = M_1 + M_2 = 11204 \text{ kip-in}$$

But the above moment need not be greater than $0.8\sum M_{pb}$. Extrapolating the beam moment at the plastic hinge location to the column face, M_{pb} is computed as follows:

$$M^*_{pd} = M_{pd} + V_{pd}\left(a + \frac{b}{2}\right)$$

$$= 6958 + 53(4.0 + 8.0) = 7594 \text{ kip} - \text{in}$$

$$0.8\sum M^*_{pb} = 0.8(2)(7594) = 12150 \text{ kip-in}$$

Therefore, the shear in the panel zone is

$$V_u = \frac{\Delta M}{0.95 d_b} - \frac{\Delta M}{h} = 497 - 78 = 419 \text{ kips}$$

The shear capacity of the panel zone is

$$\phi V_n = 0.75(0.6)(50.0)(14.66)t_p \times \left[1 + \frac{3(14.725)(1.03)^2}{(23.74)(14.66)t_p}\right]$$

Equating V_u and ϕV_n to solve for the required panel zone thickness gives t_p = 1.14 in. Since the column web thickness is 0.645 in, use a 1/2 in thick doubler plate. (The column size needs to be increased if the designer prefers not to use doubler plates.) Check Eq. 9-13 for local buckling of the doubler plate:

$$t_{(req'd)} = \frac{d_z + w_z}{90} = 0.39 \text{ in}$$

Since both the thicknesses of column web and doubler plate are larger than the required thickness, plug welds are not required to connect the doubler plate to the column web. See Figure 9.30 for the connection details.

The component of story drift produced by the panel zone deformation is computed as follows (Tsai and Popov 1990):

$$\gamma_p = \frac{V}{d_c t_p G}$$

$$= \frac{419 \times 0.94/\Omega_o}{14.66(0.645 + 0.50)29000/2.6}$$

$$= 0.00070 \text{ rad}$$

where G is the shear modulus. The story drift due to the panel zone deformation, Δ_P, is:

$$\Delta_P = 0.00070 \times 12 \times 12 = 0.10 \text{ in}$$

The total story drift produced by the column, beam, and panel zone deformations is:

$$\Delta_c + \Delta_g + \Delta_P = \frac{F_2 h(h - d_b)^2}{12EI_c} + \frac{F_2 h^2 (L - d_c)}{12EI_g} + \Delta_P$$

$$= 0.10 + 0.281 + 0.10 = 0.48 < 0.52 \text{ in} \quad \text{(OK)}$$

Note that the clear lengths are used to compute the deformations of the beams and column in the above equation.

9.5.3 Special Concentrically Braced Frames (SCBFs)

The six-story inverted-V braced frame shown in Figure 9-32 is analyzed for the loads specified earlier. The service dead load, live load, and seismic member forces, calculated taking into account load-paths and live load reduction, and maximum forces resulting from the critical load combination, are presented in Tables 9-6 and 9-7, where the axial forces and moments are expressed in kips and kip-ft,

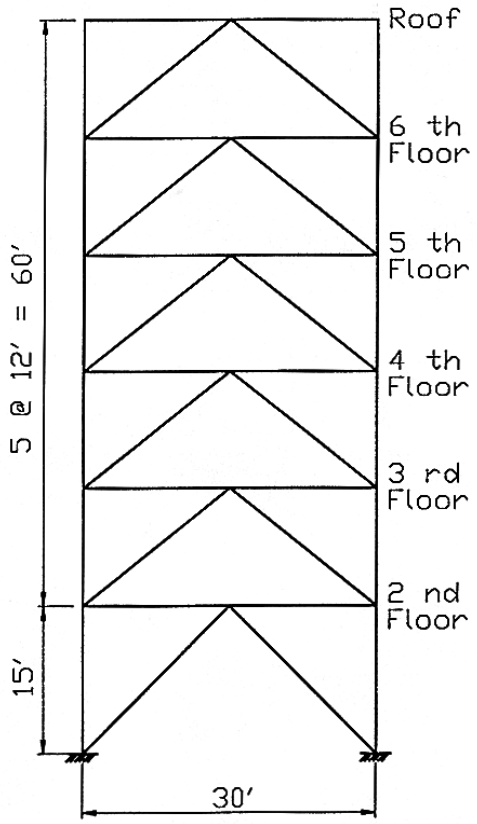

Figure 9-32. Concentrically braced frame elevation

respectively. Cladding panels are assumed connected at the columns. Note that the load combination 1.2*D*+0.5*L*+1.0*E* governs for the design of all members.

In the first phase of design (called "strength design" hereafter), members are sized without attention paid to special seismic detailing requirements, as normally done in non-seismic applications, and results are also presented in Tables 9-6 and 9-7. Members are selected per a minimum weight criterion, with beams and braces constrained to be wide-flanges sections of same width, and columns constrained to be W14 shapes continuous over two stories. ASTM A992 steel is used for all members, and the effective length factors, *K*, of 1.0 were respectively used in calculating the in-plane and out-of-plane buckling strength of braces. Additional information on the effects of end-fixity on the inelastic non-linear behavior of braces is presented elsewhere (Bruneau et al. 1997). Note that this frame geometry leads to substantial foundation uplift forces. Although not done here, increasing the number of braced bays will reduce the uplift forces.

In the second phase of design, (hereafter called "ductile design"), the seismic requirements are checked, and design is modified as necessary. The special ductile detailing requirements of braces are first checked. Here, all braces are found to have a slenderness ratio in excess of the permissible limit (Eq. 9-15), and some also violate the specified flange width-to-thickness ratio limit. For example, for the fifth story braces (W8×31), the slenderness ratio is:

$$(KL/r)_y = (1.0)(19.21)(12)/2.02$$

$$= 114.1 > 720/\sqrt{50} = 102 \qquad \text{(NG)}$$

Table 9-6. Strength design results for columns and W-shape braces (axial force in kips)

Story	P_D	P_L	P_{Lr}	P_{Q_E} or T_{Q_E}	P_u [a]	T_u [b]	Member	$\phi_c P_n$	KL/r	$b_f/2t_f$	h/t_w
Columns											
6	26.6	-	4.20	0	37	-	W14×30	190	96.6	8.7	45.4
5	66.7	10.5	4.86	29.8	132	-	W14×30	190	96.6	8.7	45.4
4	108	18.9	4.86	89	261	25	W14×53	439	75.0	6.1	30.8
3	149	26.2	4.86	172	416	90	W14×53	439	75.0	6.1	30.8
2	191	33.0	4.86	275	593	177	W14×90	1008	38.9	10.2	25.9
1	232	39.6	4.86	388	783	276	W14×90	947	48.6	10.2	25.9
Braces											
6	5.9	-	1.7	48	62	49.6	W8×24	73.7	143.2	8.1	25.8
5	7.7	4.2	-	95	120	102	W8×31	149	114.1	9.2	22.2
4	7.7	4.2	-	133	163	145	W8×35	170	113.6	8.1	20.4
3	7.7	4.2	-	164	198	180	W8×48	244	110.8	5.9	15.8
2	7.7	4.2	-	182	218	200	W8×48	244	110.8	5.9	15.8
1	6.9	3.8	-	218	257	240	W8×67	292	120.1	4.4	11.1

[a] from load combination $1.2D + 0.5L + 1.0E$ (see Eq. 9-34), where $E = \rho Q_E$.

[b] from load combination $0.9D - 1.0E$ (see Eq. 9-35).

Table 9-7. Strength design results for beams (axial force in kips, moment in kip-in)

Level	P_D	M_D	P_L	M_L	P_{Lr}	M_{Lr}	P_{Q_E} [b]	P_u [a]	M_u [a]	Section	$\phi_c P_n$	$\phi_b M_n$	KL/r	$b_f/2t_f$	h/t_w
Roof	-	11.1	-	-	-	2.0	37.2	42	16.5	W8×21	64.4	76.5	142.9	6.6	27.5
6	4.6	14.7	-	5.0	0.8	-	74.2	81	30.3	W8×24	120	87.0	111.8	8.1	25.8
5	6.0	14.8	2.1	3.3	-	-	104	113	30.4	W8×31	217	114	89.1	9.2	22.2
4	6.0	15.2	1.4	3.1	-	-	128	141	31	W8×31	217	114	89.1	9.2	22.2
3	6.1	14.9	1.2	2.9	-	-	142	156	30.6	W8×31	217	114	89.1	9.2	22.2
2	5.9	15.6	1.2	2.9	-	-	154	170	31.7	W8×31	217	114	89.1	9.2	22.2

[a] from load combination $1.2D + 0.5L + 1.0E$ (see Eq. 9-34), where $E = \rho Q_E$.

b. $M_E = 0$.

and the width-to-thickness ratio is:

$$b/t = b_f/2t_f = 9.2 > 52/\sqrt{50} = 7.35 \quad \text{(NG)}$$

These braces, therefore, have insufficient capacity to dissipate seismic energy through repeated cycles of yielding and inelastic buckling. Cold-formed square structural tubes with a specified yield strength of 46 ksi under ASTM A500 Grade B are first selected to replace the wide-flange brace sections. As shown in Table 9-8, a strength design using such hollow shapes effectively reduces brace slenderness, but does not necessarily satisfy the stringent width-to-thickness ratio limits prescribed for seismic design.

For example, for the first story braces (TS10×10×1/4), the width-to-thickness ratio is:

$$b/t = 10/0.25 = 40 > 110/\sqrt{46} = 16.22 \text{ (NG)}$$

Consequently, new brace sections are selected to comply with both the width-to-thickness and member slenderness ratio limits. These are presented in Table 9-9.

At each story, the reduced compression strength $0.8(\phi_c P_n)$ is then considered. Here, the tension brace at each level has sufficient reserve strength to compensate for the loss in compression resistance upon repeated cyclic loading, and the chosen braces are thus adequate. For example, for the TS6×6×5/8 braces at the third story,

Factored design forces: $P_u = 198$ kips
$T_u = 180$ kips

Table 9-8. Strength design results for TS-shape braces (axial force in kips)

Story	P_u[a]	T_u[b]	Member	$\phi_c P_n$	*KL/r*	*b/t*
6	62	49.6	TS6×6×3/16	88	97.7	32.0
5	120	102	TS8×8×3/16	157	72.5	42.7
4	163	145	TS9×9×3/16	178	64.2	48.0
3	198	180	TS8×8×1/4	207	73.2	32.0
2	218	200	TS9×9×1/4	253	64.8	36.0
1	257	240	TS10×10×1/4	284	64.3	40.0

[a] from load combination $1.2D + 0.5L + 1.0E$ (see Eq. 9-34), where $E = \rho Q_E$.

[b] from load combination $0.9D - 1.0E$ (see Eq. 9-35).

Table 9-9. Ductility design results for TS-shape braces (axial force in kips)

Story	P_u[a]	T_u[b]	Member	$\phi_c P_n$	*KL/r*	*b/t*
6	62	49.6	TS6×6×3/8	157	101	16.0
5	120	102	TS6×6×3/8	157	101	16.0
4	163	145	TS6×6×1/2	196	104	10.0
3	198	180	TS6×6×5/8	224	107	9.6
2	218	200	TS7×7×1/2	288	88	14.0
1	257	240	TS8×8×1/2	351	84	16.0

[a] from load combination $1.2D + 0.5L + 1.0E$ (see Eq. 9-34), where $E = \rho Q_E$.

[b] from load combination $0.9D - 1.0E$ (see Eq. 9-35).

Design strengths:

$\phi_c P_n = 224$ kips, $\phi_t T_n = \phi_t A_g F_y = 513$ kips

Reduced compression design strength:

$0.8(\phi_c P_n) = 0.8(224) = 179$ kips $< P_u = 198$ kips

Therefore, the redistributed force demand in the tension brace is:

$$T_u' = T_u + (\phi_c P_n - 0.8\phi_c P_n) = 180 + (224 - 179)$$
$$= 225 \text{ kips} < \phi_c T_n = 513 \text{ kips} \quad \text{(OK)}$$

Finally, the redundancy requirement is satisfied by checking that members in tension carry at least 30% but no more than 70% of the story shear. Note that for bays with the same number of compression and tension braces, satisfying the above member slenderness limits, this is usually not a concern. For example, check the first story brace as follows:

$$\frac{T_u / \cos\theta}{V_B} = \frac{240 / 0.707}{305} = 0.56$$

which is between 0.3 and 0.7.

Design Forces in Connections

Connections are designed to resist their expected brace tension yield force of $R_y A_g F_y$. For example, for the braces in the first story, this would correspond to a force of (1.1)(14.4)(46) = 729 kips. The brace gusset used with tubular braces usually permits out-of-plane buckling and needs to be detailed per Figure 9-15 to resist the applied axial force while undergoing large plastic rotation.

Design Forces in Columns

When $P_u/\phi_c P_n$ in columns is greater than 0.4 (as is the case here), the AISC Seismic Provisions require that columns also be designed to resist forces calculated according to the special load combinations in Eqs. 9-4 and 9-5. However, these forces need not exceed those calculated considering $1.1R_y T_n$ and $1.1R_y P_n$ of the braces. Members designed to satisfy this requirement are presented in Table 9-10.

Table 9-10. Ductility design results for columns (axial force in kips)

Story	P_u[a]	T_u[b]	$\sum P_n$[c]	$\sum T_n$[d]	Member	$\phi_c P_n$
6	34	-	34	-	W14×30	190
5	146	-	225	221	W14×30	190
4	314	80	420	465	W14×61	591
3	538	211	647	790	W14×61	591
2	796	378	886	1150	W14×109	1220
1	1078	568	1196	1543	W14×109	1147

[a] from load combination $1.2D + 0.5L \pm \Omega_o Q_E$ (see Eq. 9-4), where Ω_o =2.0.

[b] from load combination $0.9D \pm \Omega_o Q_E$ (see Eq. 9-5).

[c] $1.2D + 0.5L + \Sigma(1.1R_y P_n)$, where P_n is the brace nominal compressive strength.

[d] $1.2D + 0.5L + \Sigma(1.1R_y T_n)$, where T_n is the brace nominal tensile strength.

Cases b and d are used to check column splices and foundation uplift.

Table 9-11. Ductility design results for beams[a] (force in kips, moment in kip-in)

			Unbalanced Force							
Level	T_n	$0.3\phi_c P_n$	Vertical	Horizontal	M_{ux}	P_u	Section	$\phi_b M_{nx}$	$\phi_c P_n$	Ratio
6	372	47.3	203	1522	127	254	W30×148	1789	1172	0.90
5	372	47.3	203	1522	127	254	W30×148	1789	1172	0.90
4	479	58.7	263	1973	164	328	W30×173	2164	1765	0.96
3	524	63.0	288	2160	180	360	W30×191	2398	1956	0.94
2	570	86.4	302	2265	189	378	W30×191	2398	1956	0.99

[a] Ductility design not required at top story of a chevron braced frame per AISC Seismic provisions.

Note that columns splices would have to be designed to resist the significant uplift forces shown in this table, although the AISC Seismic Provisions indicate that the tension forces calculated in Table 9-10 need not exceed the value corresponding the uplift resistance of the foundation.

Design Forces in Beams

Finally, beams are checked for compliance with the special requirements presented in Section 9.3. Here, all beams are continuous between columns, and are braced laterally at the ends and mid-span. W30 shapes were chosen to limit beam depth.

Beams are, therefore, redesigned to resist the unbalanced vertical force induced when the compression braces are buckled and the tension braces are yielded. In this example, this substantial force governs the design. The corresponding moments and axial forces acting on the beams are shown in Table 9-11, along with the resulting new beam sizes. Note that the adequacy of these beams is checked using the AISC (1993) beam-column interaction equations.

For example, for the W30×191 beam on the second floor:

$$\frac{P_u}{2\phi_c P_n} + \left(\frac{M_{ux}}{\phi_b M_{nx}}\right) = \frac{189}{2(1956)} + \left(\frac{2265}{2398}\right)$$

$$= 0.05 + 0.94 = 0.99 < 1.0 \qquad \text{(OK)}$$

Incidentally, note that this section is a compact section.

9.5.4 Eccentrically Braced Frames (EBFs)

The configuration of the split-V-braced EBF is shown in Figure. 9-33, and the design seismic forces are listed in Table 9-5. The geometry is chosen such that the link length is about 10% of the bay width, and the inclined angle of the braces is between 35 to 60 degrees:

$e = 0.1L = 3$ ft = 36 in

$$\theta = \tan^{-1}(15/13.5) = 48° \qquad \text{(first story)}$$

$$\theta = \tan^{-1}(12/13.5) = 42° \qquad \text{(other stories)}$$

In this example, detailed design calculations are only presented for members at the first story to illustrate the procedure. Unless indicated otherwise, ASTM A992 steel is used.

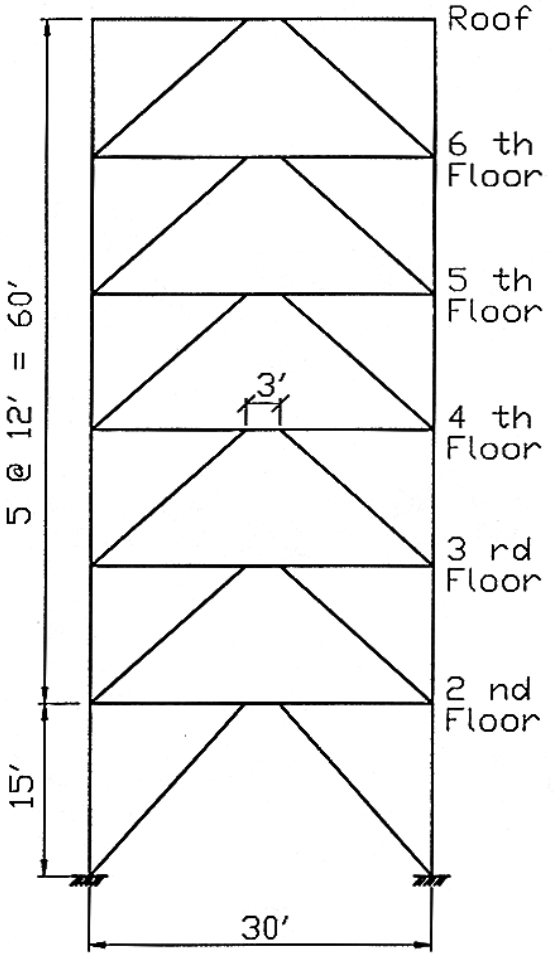

Figure 9-33. Eccentrically braced frame elevation

Link Design

Shear links with $e \le 1.6\ M_p/V_p$ are used to achieve higher structural stiffness and strength. The AISC Seismic Provisions stipulate that the beam outside the link shall be able to resist the forces generated by at least 1.1 times the expected nominal shear strength of the link. Assuming that the braces are rigidly connected to the link, that the beam can resist 95% of the link end moment, and that the beam flexural capacity is reduced by 30% due to the presence of an axial force:

$$(0.7)R_y(\phi_b M_p) \ge 0.85(1.1)R_y V_n(e/2)$$

or

$$1.35M_p/V_n \ge e$$

For shear links, the above requirement for the maximum link length is more stringent than $1.6M_p/V_p$. The required strengths for the link on the second floor are

$$V_u = 1.4D + 0.5L + E$$
$$= 1.4(1.1) + 0.5(0.4) + 98.0 = 100 \text{ kips}$$
$$M_u = 1.4D + 0.5L + E$$
$$= 1.4(8.0) + 0.5(3.0) + 98(3.0/2) \qquad = 160 \text{ kip-ft}$$

Note that there is no axial force acting on the shear links (i.e., $P_u = 0$ kip). Illustrating this procedure for the shear link on the second floor:

$$1.35M_p/V_p \ge 36 \text{ in} \Rightarrow M_p/V_p \ge 26.7 \text{ in}$$
$$V_u = 100 \text{ kips} \le \phi V_n = \phi V_p$$
$$= 0.9(0.6)(50)t_w(d - 2t_f)$$
$$\Rightarrow t_w(d - 2t_f) \ge 3.70 \text{ in}^2$$
$$V_u = 100 \text{ kips} \le \phi V_n = \phi(2M_p/e)$$
$$= 2(0.9)(50Z_x)/36 \Rightarrow Z_x \ge 40.0 \text{ in}^3$$

Based on the above three requirements, select a W12×45 section for the link:

$$Z_x = 64.7 \text{ in}^3 > 40.0 \text{ in}^3 \qquad \text{(OK)}$$

$$t_w(d - 2t_f) = 3.87 \text{ in}^2 > 3.70 \text{ in}^2 \qquad \text{(OK)}$$

$$\frac{M_p}{V_p} = \frac{Z_x}{0.6(d - 2t_f)t_w} = 27.9 \text{ in} > 26.7 \text{ in} \qquad \text{(OK)}$$

$$\frac{b_f}{2t_f} = 7.0 < \frac{52}{\sqrt{F_y}} = 7.4 \qquad \text{(OK)}$$

$$\frac{h}{t_w} = 29.0 < \frac{520}{\sqrt{F_y}} = 73.5 \qquad \text{(OK)}$$

$$V_n = \min\left\{V_p, 2M_p/e\right\} = \min\left\{116, 180\right\} = 116 \text{ kips} \qquad \text{(OK)}$$

Beam Outside of Link

The moment at both ends of the link is:

$$M_u = 1.1(R_y V_n e/2) = 1.1(1.1\times 116\times 3.0/2) = 211 \text{ kip-in}$$

This moment is resisted by both the rigidly connected brace and the beam outside the link. Assuming that the beam resists 85% of the link moment, the beam end moment including the gravity load effect (M_D = 8 kip-ft, M_L = 3 kip-ft) is

$$M_u = 0.85(211) + 1.2(8.0) + 0.5(3.0) = 190 \text{ kip-ft}$$

The axial force ratio in the beam is

$$\frac{P_u}{\phi_b P_y} = \frac{126}{0.9A_g F_y} = 0.212 > 0.125$$

Checking the beam web local buckling (see Table 9-2):

$$\lambda_{ps} = \frac{191}{\sqrt{F_y}}\left(2.33 - \frac{P_u}{\phi_b P_y}\right) \geq \frac{253}{\sqrt{F_y}} = 57.2$$

$$\lambda = \frac{h}{t_w} = 16.7 < \lambda_{ps} \qquad \text{(OK)}$$

Checking the strength of the beam segment as a beam-column:

$$\left[L_p = 6.9 \text{ ft}\right] < \left[L_b = 13.5 \text{ ft}\right] < \left[L_r = 20.3 \text{ ft}\right]$$

$$\phi_b M_p = 243, \quad BF = 5.07, \quad C_b \approx 1.67$$

$$\phi_b M_n = C_b\left[\phi_b M_p - BF\left(L_b - L_p\right)\right] = 350 \geq \phi_b M_p$$

Use $\phi_b M_n = 243$ kip-ft

$$P_{e1} = \frac{\pi^2 EI_x}{(KL_x)^2} = 3817 \text{ kips}$$

$$C_m = 0.85$$

$$B_1 = \frac{C_m}{1 - \frac{P_u}{P_{e1}}} = \frac{0.85}{1 - \frac{126}{3817}} = 0.88 < 1.0$$

Use B_1 = 1.0

$$(KL)_y = 13.5 \text{ ft}, \quad \phi_c P_n = 337 \text{ kips}$$

$$\frac{P_u}{R_y(\phi_c P_n)} + \frac{8}{9}\frac{B_1 M_u}{R_y(\phi_b M_n)} = 0.34 + 0.63 = 0.97 < 1.0 \qquad \text{(OK)}$$

Diagonal Brace

To compute the beam shear, V_b, assume the beam moment at the column end is zero.

$$1.25R_y V_n = 160 \text{ kips}$$

$$1.25R_y V_n\left(e/2\right) = 240 \text{ kip-ft}$$

$$V_b = \frac{1.25R_y V_n\left(e/2\right)}{L_b} = 18 \text{ kips}$$

Therefore, the brace force including the gravity load effect (V_D = 5.7 kips, V_L = 2.2 kips) is

$$P_u = (1.25R_y V_n + V_b + 1.2V_D + 0.5V_L)/\sin(\theta) = 250 \text{ kips}$$

The brace length is 20.2 ft. Selecting a square tubular section TS8×8×1/2 (A500 Grade B steel):

$$\phi_c P_n = 366 \text{ kips} > 250 \text{ kips} \qquad \text{(OK)}$$

$b/t = 6.5/0.5 = 13 < \lambda_p = 190/\sqrt{F_y} = 28$ (OK)

Once the brace size is determined, it is possible to determine the link end moment based on the relative stiffness (I/L) of the brace and the beam segment outside the link. The moment distribution factor is

$$(DF)_{br} = \frac{I_{br}/L_{br}}{I_{br}/L_{br} + I_b/L_b} = 0.20$$

Therefore, the moment at the end of brace is

$$M_u = 240 \times (DF)_{br} = 48 \text{ kip-ft}$$

The brace capacity is checked as a beam-column:

$$\phi_b M_n = \phi_b (Z_x F_y) = 137 \text{ kip-ft}$$

$$\frac{P_u}{\phi_c P_n} + \frac{8}{9}\frac{M_u}{\phi_b M_n} = 0.68 + 0.31$$
$$= 0.99 < 1 \quad \text{(OK)}$$

Link Rotation

The axial force produced by the design seismic force in the first story is

$$P = 88/\cos(\theta) = 132 \text{ kips}$$

The axial deformation of the brace is

$$\Delta = \frac{PL}{EA} = \frac{132(20.2\times12)}{29000(14.4)} = 0.077 \text{ in}$$

The elastic story drift is

$$\delta_e = \frac{\Delta}{\cos(\theta)} = 0.115 \text{ in}$$

and the design story drift is

$$\delta_s = C_d \delta_e / I = 4.0(0.115)/1.0 = 0.46 \text{ in}$$

Therefore, the link rotation is

$$\gamma_p = \frac{L}{e}\left(\frac{\delta_s}{h}\right) = \frac{30.0}{3.0}\left(\frac{0.46}{15\times12}\right) = 0.026 \text{ rad}$$

The link rotation capacity is 0.08 rad because the link length (= 36 in) is smaller than 1.6 M_p/V_p (= 44.6 in). Thus, the link deformation capacity is sufficient.

Lateral Bracing

Full-depth stiffeners of A36 steel are to be used in pairs at each end of the links. The required thickness of these stiffeners is

t = max {0.75t_w, 3/8} = 3/8 in

Lateral bracing similar to that shown in Figure 9-31 is needed for the links, except that the bracing needs to be designed for 6% of the expected link flange force, $R_y F_y b_f t_f$.

Link Stiffeners

One-sided intermediate stiffeners are permitted because the link depth is less than 25 inches. The required thickness is

t = max {t_w , 3/8} = 3/8 in

The required stiffener spacing, a, is based on Eq. 9-28, where C_B is (see Figure 9-25):

$$C_B = 59.3 - 367\gamma_P = 50.1$$

$$a = C_B t_w - \frac{d}{5} = 14.4 \text{ in}$$

Therefore, three intermediate stiffeners are provided.

The weld between the stiffener and the link web should be designed to resist the following force:

$F = A_{st} F_y$ = (3.75)(0.375)(36) = 51 kips

The required total design force between the stiffener and the flanges is

$F = A_{st} F_y/4$ = 12.8 kips

A minimum fillet weld size of ¼ in. satisfies the above force requirement.

Columns

Table 9-12. Summary of member sizes and column axial loads

Floor Level	Link Size	$\Sigma 1.1R_yV_n$ (kips)	ΣP_D (kips)	ΣP_L (kips)	Column Size	Brace Size
R	W10×45					
		113	30	5	W12×40	TS8×8×½
6	W10×45					
		226	71	14	W12×40	TS8×8×½
5	W10×45					
		339	112	22	W12×72	TS8×8×½
4	W10×45					
		452	153	29	W12×72	TS8×8×½
3	W12×45					
		592	194	35	W12×106	TS8×8×½
2	W12×45					
		732	235	42	W12×106	TS8×8×½

Columns must be designed to satisfy the special load combination presented in Eq. 9-4, where $\Omega_o E$ is replaced by the seismic force generated by 1.1 times the expected nominal strength (R_yV_n) of the links. The column axial load produced by both gravity loads and seismic forces are listed in Table 9-12. The required axial compressive strength is

$$P_u = 1.2(235) + 0.5(42) + 732 = 1035 \text{ kips}$$

A W12×106 column, with a design axial load capacity of 1040 kips, is chosen for the lowest two stories. The column splice must be designed for the tensile force determined from the load combination in Eq. 8.5:

$$P_u = 0.9D - \Omega_o Q_E = 0.9(235) - 732$$

$$= -521 \text{ kips}$$

As stated in the SCBF design example, using more than one braced bay in the bottom stories may reduce the tensile force in the columns and increase the overturning resistance of the building.

REFERENCES

9-1 AIJ, *Performance of Steel Buildings during the 1995 Hyogoken-Nanbu Earthquake* (in Japanese with English summary), Architectural Inst. of Japan, Tokyo, Japan, 1995.

9-2 AISC, *Load and Resistance Factor Design Specification for Structural Steel Buildings*, AISC, Chicago, IL, 1993.

9-3 AISC, *Specifications for Structural Steel Buildings,* AISC, Chicago, IL, 1989.

9-4 AISC, *Near the Fillet of Wide Flange Shapes and Interim Recommendations*, Advisory Statement on Mechanical Properties, AISC, Chicago, IL, 1997a.

9-5 AISC, *Seismic Provisions for Structural Steel Buildings,* with Supplement No. 1 (1999), AISC, Chicago, IL, 1992 and 1997b.

9-6 ASCE, *Minimum Design Loads for Buildings and Other Structures*, ASCE Standard 7-98, ASCE, New York, NY, 1998.

9-7 Astaneh-Asl, A., Goel, S.C., Hanson, R.D., "Earthquake-resistant Design of Double Angle Bracings," *Engrg. J.*, Vol. 23, No. 4, pp. 133-147, AISC, 1981.

9-8 Becker, R., "Seismic Design of Steel Buildings Using LRFD," in *Steel Design Handbook* (editor: A. R. Tamboli), McGraw-Hill, 1997.

9-9 Bruneau, M., Mahin, S.A., "Ultimate Behavior of Heavy Steel Section Welded Splices and Design Implications," *J. Struct. Engrg.*, Vol. 116, No. 8, pp. 2214-2235, ASCE, 1990.

9-10 Bruneau, M., Uang, C.M, Whittaker, A., *Ductile Design of Steel Structures*, McGraw Hill, New York, NY, 1997.

9-11 BSSC, *NEHRP Recommended Provisions for the Development of Seismic Regulations for New Buildings*, Federal Emergency Management Agency, Washington, DC, 1997.

9-12 Chen, S.J., Yeh, C.H. and Chu, J.M., "Ductile Steel Beam-Column Connections for Seismic Resistance," *J. Struct. Engrg.*, Vol. 122, No. 11, pp. 1292-1299. ASCE, 1996.

9-13 Chi, B. and Uang, C.M., "Seismic Retrofit Study on Steel Moment Connections for the Los Angeles Department of Public Works Headquarters Building," *Report No. TR-2000/14*, Department of Structural Engineering, University of California, San Diego, La Jolla, CA, 2000.

9-14 Engelhardt, M. D. and Popov, E. P., "On Design of Eccentrically Braced Frames," *Earthquake Spectra*, Vol. 5, No. 3, pp. 495-511, EERI, 1989.

9-15 Engelhardt, M.D. and Sabol, T., "Reinforcing of Steel Moment Connections with Cover Plates: Benefits and Limitations," *Engrg. J.*, Vol. 20, Nos. 4-6, pp. 510-520, 1998.

9-16 Engelhardt, M.D., Winneburger, T., Zekany, A.J., and Potyraj, T.J., "The Dogbone Connection: Part II," *Modern Steel Construct.*, Vol. 36. No. 8, pp. 46-55, AISC, 1996.

9-17 Fujimoto, M., Aoyagi, T., Ukai, K., Wada, A., and K. Saito, "Structural Characteristics of Eccentric K-Braced Frames," *Trans.*, No. 195, pp. 39-49, AIJ, May 1972.

9-18 Gilton, C., Chi, B., and Uang, C.-M., "Cyclic Response of RBS Moment Connections: Weak-Axis Configuration and Deep Column Effects," *Report No. SSRP-2000/03*, Department of Structural Engineering, University of California, San Diego, La Jolla, CA, 2000.

9-19 Gross, J. L., Engelhardt, M. D., Uang, C.-M., Kasai, K., and N. Iwankiw, *Modification of Existing Welded Steel Moment Frame Connections for Seismic Resistance*, Steel Design Guide Series 12, AISC and NIST, 1998.

9-20 Hamburger, R. "More on Welded Connections," *SEAONC News*, Structural Engineers Association of Northern California, San Francisco, CA, April, 1996.

9-21 Hjelmstad, K. D. and Popov, E. P., "Characteristics of Eccentrically Braced Frames," *J. Struct. Engrg.*, Vol. 110, No. 2, pp. 340-353, ASCE, 1984.

9-22 Hjelmstad, K. D. and Popov, E. P., "Cyclic Behavior and Design of Link Beams," *J. Struct. Engrg.*, Vol. 109, No. 10, pp. 2387-2403, ASCE, 1983.

9-23 ICBO, *Uniform Building Code*, Int. Conf. of Building Officials, Whittier, CA, 1988.

9-24 Iwankiw, R.N. and Carter, C.J., "The Dogbone: A New Idea to Chew On," *Modern Steel Construct.*, Vol. 36. No. 4, pp. 18-23, AISC, Chicago IL, 1996.

9-25 Jokerst, M. S. and Soyer, C., "San Francisco Civic Center Complex: Performance Based Design with Passive Dampers and Welded Steel Frames," *Proc.*, 65th Annual Convention, pp. 119-134, SEAOC, 1996.

9-26 Kasai, K. and Popov, E. P., "On Seismic Design of Eccentrically Braced Frames," *Proc.*, 8th World Conf. Earthquake Engrg., Vol. V, pp. 387-394, IAEE, San Francisco, 1985.

9-27 Kasai, K. and Popov, E. P., "Cyclic Web Buckling Control for Shear Link Beams," *J. Struct. Engrg.*, Vol. 112, No. 3, pp. 505-523, ASCE, 1986a.

9-28 Kasai, K. and Popov, E. P., "General Behavior of WF Steel Shear Link Beams," *J. Struct. Engrg.*, Vol. 112, No. 2, pp. 362-382, ASCE, 1986b.

9-29 Krawinkler, H., Bertero, V.V., and Popov, E.P., "Inelastic Behavior of Steel Beam-Column Subassemblages," *Report No. UCB/EERC-71/7*, Univ. of Calif., Berkeley, Berkeley, CA, 1971.

9-30 Krawinkler, H., Bertero, V.V., and Popov, E.P., "Shear Behavior of Steel Frame Joints," *J. Struct. Div.*, Vol. 101, ST11, pp. 2317-2338. ASCE, 1975.

9-31 Libby, J. R., "Eccentrically Braced Frame Construction–A Case Study," *Engrg. J.*, Vol. 18, No. 4, pp. 149-153, AISC, 1981.

9-32 Malley, J. O. and Popov, E. P., "Shear Links in Eccentrically Braced Frames," *J. Struct. Engrg*., Vol. 110, No. 9, pp. 2275-2295, ASCE, 1984.

9-33 Manheim, D. N. and Popov, E. P., "Plastic Shear Hinges in Steel Frames," *J. Struct. Engrg*., Vol. 109, No. 10, pp. 2404-2419, ASCE, 1983.

9-34 Merovich, A., Nicoletti, J. P., and Hartle, E., "Eccentric Bracing in Tall Buildings," *J. Struct. Div*., Vol. 108, No. ST9, pp. 2066-2080, ASCE, 1982.

9-35 Nakashima, M. And Wakabayashi, M., "Analysis and Design of Steel Braces and Braced Frames," in *Stability and Ductility of Steel Structures under Cyclic Loading*, pp. 309-322, CRC Press, 1992.

9-36 Noel, S. and Uang, C.-M., "Cyclic Testing of Steel Moment Connections for the San Francisco Civic Center Complex," *Report No. TR-96/07*, Univ. of California, San Diego, La Jolla, CA, 1996.

9-37 Plumier, A., "New Idea for Safe Structures in Seismic Zones," *Proc.,* Symposium of Mixed Structures Including New Materials, pp. 431-436, IABSE, Brussels, Belgium, 1990.

9-38 Redwood, R.G., and Channagiri, V.S., "Earthquake-Resistant Design of Concentrically Braced Steel Frames," *Canadian J. Civil Engrg.*, Vol. 18, No. 5, pp. 839-850, 1991.

9-39 Ricles, J. M. and Popov, E. P., "Composite Action in Eccentrically Braced Frames," *J. Struct. Engrg*., Vol. 115, No. 8, pp. 2046-2065, ASCE, 1989.

9-40 Roeder, C. W. and Popov, E. P., "Eccentrically Braced Steel Frames For Earthquakes," *J. Struct. Div*., Vol. 104, No. ST3, pp. 391-411, ASCE, 1978.

9-41 Roeder, C. W., Foutch, D. A., and Goel, S. C., "Seismic Testing of Full-Scale Steel Building–Part II," *J. Struct. Engrg*., Vol. 113, No. 11, pp. 2130-2145, ASCE, 1987.

9-42 SAC, "Interim Guidelines: Evaluation, Repair, Modification, and Design of Welded Steel Moment Frame Structures," *Report FEMA No. 267/SAC-95-02*, SAC Joint Venture, Sacramento, CA, 1995.

9-43 SAC, "Interim Guidelines Advisory No. 1, Supplement to FEMA 267*," Report No. FEMA 267A/SAC-96-03*, SAC Joint Venture, Sacramento, CA, 1997.

9-44 SAC, "Technical Report: Experimental Investigations of Beam-Column Subassemblages, Parts 1 and 2," *Report No. SAC-96-01*, SAC Joint Venture, Sacramento, CA, 1996.

9-45 SAC, "Recommended Seismic Design Criteria for New Moment-Resisting Steel Frame Structures," *Report No. FEMA* 350, SAC Joint Venture, Sacramento, CA, 2000.

9-46 Shibata, M., Nakamura T., Yoshida, N., Morino, S., Nonaka, T., and Wakabayashi, M., "Elastic-Plastic Behavior of Steel Braces under Repeated Axial Loading," *Proc*., 5th World Conf. Earthquake Engrg., Vol. 1, pp. 845-848, IAEE, Rome, Italy, 1973.

9-47 SSPC, *Statistical Analysis of Tensile Data for Wide-Flange Structural Shapes*, Chaparral Steel Co., Midlothian, TX, 1994.

9-48 Tanabashi, R., Naneta, K., and Ishida, T., "On the Rigidity and Ductility of Steel Bracing Assemblage," *Proc.*, 5th World Conf. Earthquake Engrg., Vol. 1, pp. 834-840, IAEE, Rome, Italy, 1974.

9-49 Teal, E. J., "Seismic Drift Control Criteria," *Engrg. J*., Vol. 12, No. 2, pp. 56-67, AISC, 1975.

9-50 Teal, E., *Practical Design of Eccentric Braced Frames to Resist Seismic Forces*, Struct. Steel Res. Council, CA, 1979.

9-51 Tremblay, R., Bruneau, M., Nakashima, M., Prion, H.G.L., Filiatrault, M., DeVall, R., "Seismic Design of Steel Buildings: Lessons from the 1995 Hyogo-ken Nanbu Earthquake", *Canadian J. Civil Engrg.*, Vol. 23, No. 3, pp. 757-770, 1996.

9-52 Tremblay, R., Timler, P., Bruneau, M., Filiatrault, A., "Performance of Steel Structures during the January 17, 1994, Northridge Earthquake," *Canadian J. Civil Engrg.*, Vol. 22, No. 2, pp. 338-360, 1995.

9-53 Tsai, K.-C., and Popov, E.P., "Seismic Panel Zone Design Effects on Elastic Story Drift of Steel Frames," *J. Struct. Engrg*., Vol. 116, No. 12, pp. 3285-3301, ASCE, 1990.

9-54 Tsai, K.-C., and Popov, E.P., "Steel Beam-Column Joints in Seismic Moment-Resisting Frames," *Report No. UCB/EERC-88/19*, Univ. of Calif., Berkeley, 1988.

9-55 Yu, Q.S., Uang, C.M., and Gross, J., "Seismic Rehabilitation Design of Steel Moment Connection with Welded Haunch," *Journal of Structural Engineering*, Vol. 126, No. 1, pp. 69-78, ASCE, 2000.

9-56 Uang, C.-M. "Establishing R (or R_w) and C_d Factors for Building Seismic Provisions," *J. Struct. Engrg*., Vol. 117, No. 1, pp. 19-28, ASCE, 1991.

9-57 Uang, C.-M. and Noel, S., "Cyclic Testing of Strong- and Weak-Axis Steel Moment Connection with Reduced Beam Flanges," *Report No. TR-96/01*, Univ. of Calif., San Diego, CA, 1996.

9-58 Uang, C.-M and Fan, C.C, "Cyclic Stability of Moment Connections with Reduced Beam Section," *Report No. SSRP-99/21*, Department of Structural Engineering, University of California, San Diego, La Jolla, CA, 1999.

9-59 Whittaker, A. S., Uang, C.-M., and Bertero, V. V., "Seismic Testing of Eccentrically Braced Dual Steel Frames," *Earthquake Spectra*, Vol. 5, No. 2, pp. 429-449, EERI, 1989.

9-60 Whittaker, A.S. and Gilani, A., "Cyclic Testing of Steel Beam-Column Connections," *Report No. EERC-STI/96-04*, Univ. of Calif., Berkeley, 1996.

9-61 Whittaker, A.S., Bertero V.V., and Gilani, A.S. "Evaluation of Pre-Northridge Steel Moment-

Resisting Joints." *Struct. Design of Tall Buildings*. Vol. 7, No. 4, pp. 263-283, 1998.

9-62 Yang, M.-S., "Shaking Table Studies of an Eccentrically Braced Steel Structure," *Proc.*, 8th World Conf. Earthquake Engrg., Vol. IV, pp. 257-264, IAEE, San Francisco, CA, 1985.

9-63 Zekioglu, A., Mozaffarian, H., Chang, K.L., Uang, C.-M., and Noel, S., "Designing after Northridge", *Modern Steel Construct.*, Vol. 37. No. 3, pp. 36-42, AISC, 1997.